

MicroRNA dysregulation in pulmonary arteries from COPD: Relationships with vascular remodeling

Melina M. Musri^{1,2*#}, Núria Coll-Bonfill^{1,3*}, Bradley A. Maron^{4¶}, Víctor I. Peinado^{1,3¶}, Ruisheng Wang⁴, Jordi Altirriba⁵, Isabel Blanco^{1,3}, William M. Oldham⁶, Olga Tura-Ceide^{1,3}, Jessica García-Lucio¹, Benjamin de la Cruz-Thea², Gunter Meister⁷, Joseph Loscalzo⁴ and Joan A. Barberà^{1,3}.

*,¶ These authors contributed equally to this work.

1. Department of Pulmonary Medicine, Hospital Clínic, *Institut d'Investigacions Biomèdiques Agustí Pi i Sunyer*, University of Barcelona, Barcelona, Spain.
2. *Instituto de Investigación Médica Mercedes y Martín Ferreyra*, INIMEC-CONICET, Universidad Nacional de Córdoba, Córdoba, Argentina.
3. Biomedical Research Networking Center for Respiratory Diseases (CIBERES), Madrid, Spain.
4. Division of Cardiovascular Medicine, Department of Medicine, Brigham and Women's Hospital, Boston, MA, USA.
5. Laboratory of Metabolism, Department of Internal Medicine Specialties, Faculty of Medicine, University of Geneva, Geneva, Switzerland
6. Pulmonary and Critical Care Medicine Division, Department of Medicine, Brigham and Women's Hospital, Boston, MA, USA.
7. Biochemistry Center Regensburg (BZR), Laboratory for RNA Biology, University of Regensburg, Regensburg, Germany.

#Corresponding author:

Melina M. Musri, PhD, IDIBAPS, Hospital Clínic, Villarroel, 170. 08036-Barcelona, Spain. Phone/Fax: (34) 93 227 54 04. E-mail: mmusri@clinic.ub.es; mmusri@imbf.uncor.edu

MMM, NCB, VIP and JAB contributed to the conception and design of the study, the analysis and interpretation of data and the writing of the manuscript. BAM, VIP, RSW, JA, JAB, IB, WO, OTC, JGL, BCT, GM, JL contributed in the analysis and interpretation of data. JL, JA, GM and BAM also contributed in revising the manuscript.

Supported by grants from the *Instituto de Salud Carlos III* (ISCiii) (PI 09/00536 and PI 13/00836); Spanish Society of Respiratory Medicine (SEPAR-2009); Fundación Contra la

Hipertensión Pulmonar (FCHP); National Institutes of Health (NIH) (1K08HL11207-01A1, 1K08128802-01A1, HL061795, HL108630, HG007690 and GM107618); American Heart Association (AHA) (15GRNT25080016); Pulmonary Hypertension Association; Cardiovascular Medical Research and Education Fund (CMREF); Klarman Foundation at Brigham and Women's Hospital; and the American Thoracic Association (ATS) Foundation. MMM was the recipient of a Sara Borrell contract from the ISCiii; JGL was the recipient of a Pre-doctoral contract from the ISCiii; OTC was the recipient of Marie-Curie Biotrack grant; and BCT is the recipient of a Pre-doctoral contract from CONICET.

Running head: miRNAs in vascular remodeling associated with COPD

Subject category: vascular smooth muscle (3.15), cell fate, vascular: proliferation (3.28), COPD pathogenesis (9.13), vascular remodelling (17.10)

Word count: 3382

At a Glance Commentary

Scientific Knowledge on the subject:

The molecular mechanisms underlying pulmonary vascular changes in COPD are not fully understood. MicroRNAs (miRNAs) are small non-coding RNAs that regulate mRNA expression levels modulating cell phenotypes. There is no information on the potential role of miRNA dysregulation on the development of pulmonary vascular remodeling, which is frequently observed in COPD.

What this study adds to the field:

In pulmonary artery specimens from COPD patients we found alteration of miRNA expression, including the downregulation of miR-197. MiR-197 expression correlated with the severity of both pulmonary vascular remodeling and airflow obstruction. In vitro, miR-197 regulates smooth muscle cell proliferation targeting, among others, the proliferative transcription factor E2F1. The current findings provide new clues for a better understanding of the mechanisms underlying pulmonary vascular disease in COPD.

This article has an online data supplement, which is accessible from this issue's table of content online at www.atsjournals.com.

ABSTRACT

Background: Pulmonary vascular remodeling is an angiogenic-related process involving changes in smooth muscle cell (SMC) homeostasis, which is frequently observed in chronic obstructive pulmonary disease (COPD). MicroRNAs (miRNAs) are small non-coding RNAs that regulate mRNA expression levels of many genes leading to the manifestation of cell identity and specific cellular phenotypes. Here we evaluate the miRNA expression profiles of pulmonary arteries (PA) of patients with COPD and its relationship with the regulation of SMC phenotypic change.

Methods and results: miRNA expression profiles from PA of 12 COPD patients, 9 smokers with normal lung function (SK), and 7 non-smokers (NS) were analyzed using TaqMan Low Density Arrays. In COPD patients, expression levels of miR-98, miR-139-5p, miR-146b-5p and miR-451 were upregulated, as compared with NS. In contrast, miR-197, miR-204, miR-485-3p, and miR-627 were downregulated. MiRNA-197 expression correlated with both airflow obstruction and PA intimal enlargement. In an *in vitro* model of SMC differentiation, miR-197 expression was associated with a SMC contractile phenotype. MiR-197 inhibition blocked the acquisition of contractile markers in SMC and promoted a proliferative/migratory phenotype measured by both cell cycle analysis and wound-healing assay. Using luciferase assays, western blot, and qPCR we confirmed that miR-197 targets the transcription factor E2F1. In PA from COPD patients, levels of E2F1 were increased, as compared with NS.

Conclusions: In PA of COPD patients, remodeling of the vessel wall is associated with downregulation of miR-197, which regulates SMC phenotype. The effect of miR-197 on PA might be mediated, at least in part, by the key pro-proliferative factor E2F1.

Word count: 250

Key words: vascular remodeling, smooth muscle cell phenotypic switch, miRNAs, pulmonary artery, COPD.

INTRODUCTION

Pulmonary vascular remodeling is a characteristic feature of chronic obstructive pulmonary disease (COPD) and is considered the principal determinant of pulmonary hypertension (PH) (1) (2). Intimal proliferation of dedifferentiated vascular smooth muscle cells (SMC) is the main cellular contributor to pulmonary vessel remodeling (intimal hyperplasia) in COPD (3). Other cell populations might also contribute to the enlargement of the intima (4, 5, 6). The molecular mechanisms underlying pulmonary vascular cell dysfunction including SMC proliferation, in this clinical setting are poorly understood.

MicroRNAs (miRNAs) are an evolutionarily conserved 21-nucleotide (nt) class of small noncoding RNAs involved in a number of cellular processes. MiRNAs bring the RNA-induced silencing complex (RISC) to a specific target mRNA by binding to complementary sites within the 3' untranslated regions (UTRs) and promoting its translational repression and/or degradation (7).

Recent studies show that miRNAs modulate the cell fate of both SMC and endothelial cells (EC) in vessel remodeling (8, 9, 10). Specifically, miR-143/145 regulates SMC differentiation and is necessary to maintain a contractile phenotype (11). Its expression is reduced in plexiform lesions of pulmonary arterial hypertension (PAH) (12), and its downregulation promotes the proliferation of neointimal cells after vascular injury, whereas restoration of miR-145 expression reverses intimal growth (13). MiR-204 is also downregulated in plexiform lesions, (12) explanted lungs (14), and plasma of PAH patients (15). MiR-204 acts as a negative regulator of SMC proliferation (14). By contrast, miR-21 and miR-126 are upregulated in the plexiform lesions of PAH (12) and in experimental models of PH (11),

while the expression of miR-17-92 in human pulmonary artery SMC is downregulated in PAH (16, 17). MiR-21 has been shown to regulate both SMC proliferation and differentiation (18). MiR-126 induces SMC differentiation, and miR-17-92 maintains a differentiated SMC phenotype (16). Alteration of the miRNA expression profile has also been found in lungs of rats and in human airway epithelium exposed to cigarette smoke (16, 19), as well as in COPD patients (20, 21), underscoring the potential role of these molecules in the regulation of pulmonary vascular remodeling in these conditions.

MiRNA expression is tissue-specific, and every cell type contains specific miRNA profiles that help to establish and maintain distinctive gene expression signatures. We hypothesized that miRNAs might contribute to the pathogenesis of pulmonary vascular remodeling in COPD, specifically by modulating SMC phenotype. Accordingly, the present study aimed to identify miRNAs that mediate cell proliferation in pulmonary arteries (PA) obtained from lung tissue samples of COPD patients and control subjects.

MATERIAL AND METHODS (word count 498)

Detailed descriptions of methods are provided in the online supplement.

Patient characteristics

PA segments from surgical lung resection patients, collected over 2 years, with localized lung neoplasms were evaluated. Twelve patients were diagnosed with COPD, nine patients were current smokers with normal lung function (SK), and the remaining seven patients were nonsmokers with normal lung function (NS) (Table 1). The study was approved by the Ethics Committee of the Hospital Clinic, Barcelona, Spain.

MicroRNA expression in pulmonary arteries

RNA isolation of pulmonary arteries was performed using Trizol (Invitrogen). The retrotranscription was performed using 10 ng of total RNA using the Taqman[©] miRNA reverse transcription kit and megaplex[™] pools of RT primers (Applied Biosystems) according to the manufacturer's instructions. Taqman[©] Low density array human miRNA cards A&B set v3.0 (TLDA, Applied Biosystems) was used to analyze expression of 381 miRNAs.

Cell differentiation experiments

We studied a cellular model of SMC differentiation triggered by cell-to-cell contact and cell confluency as previously described (22).

Immunofluorescence

SMC differentiation was assessed by immunofluorescence, as previously described (22, 23). The primary antibodies used were directed against α -SMA (1/750), calponin (1/75; DAKO Cytomation, Carpinteria, CA). An antibody against antigen Ki-67 (1/50; Novocastra[®], Newcastle, UK) was used to measure cell proliferation.

Gene Expression analysis

To study mRNA expression, RNA isolation followed by real time RT-PCR was performed. MiRNA expression was analyzed by northern blot, and protein expression was evaluated using western blot.

Functional in vitro assays in SMC cultures

These studies included analysis of cell migration by wound healing assays, the use 2' O-methyl antisense oligonucleotides chemically synthesized (Pierce) to inhibit miRNA, and luciferase assays to demonstrate miRNA-197 target binding.

Study design

MicroRNA expression of PA from patients was analyzed. *Limma* and a gene network analysis to evaluate the miRNA signature and its associated interactome was performed. Among the dysregulated miRNAs, miR-98, miR-451 and miR-197 correlated with spirometric measurements and vascular remodeling, but only miR-197, which is related to cell proliferation in other cell systems, had not previously been studied in SMC or intima hyperplasia. By using bioinformatics inference, we found that miR-197 targets cell proliferation related genes. Next, miR-197 function was evaluated in an *in vitro* model of SMC differentiation. Finally, to find new insights into the mechanism by which miR-197 regulates proliferation, expression of the plausible target E2F1 was analyzed in SMC after miRNA inhibition with antisense 2'O- methylated RNA oligos and in PA.

Statistical analysis

All values are reported as mean±SEM. Measurements were performed in duplicate, and at least three independent experiments were performed for each set of conditions. Two-group comparisons were analyzed using the two-tailed paired Student *t*-test for dependent samples (paired measurements for one set of items) or the Mann–Whitney Rank Sum test for non-normally distributed data. Group comparisons were performed using one-way ANOVA. Post hoc pairwise comparisons were made using the Student Newman–Keuls test for normally

distributed variables or the Kruskal–Wallis and Dunn tests for non-normally distributed variables. For all procedures, P -values <0.05 were considered statistically significant.

RESULTS

Differential expression of miRNAs in pulmonary arteries

We analyzed the expression of 381 miRNAs in pulmonary artery homogenates isolated from COPD, SK, and NS lung tissue samples using Taqman Low Density Arrays (TLDA, Apply Biosystems). After differential expression analysis, obtained by applying *limma* to the miRNA expression data, we found that COPD patients showed upregulation of miR-98, miR-139-5p, miR-146b-5p, and miR-451, and downregulation of miR-197, miR-204, miR-485-3p, and miR-627 when compared with NS (Table 2 and Figure 1; Table E1, Figure E1 and Figure E2). Interestingly, pulmonary arteries from SK displayed a similar miRNA expression pattern as in COPD, although they did not achieve statistical significance (Table 2, Figure 1 and Figure E2).

Deregulated miRNA in COPD target a number of genes related to proliferation

Each miRNA has a large number of targets according to the TargetScan database. We focused on those targets with functions in cell proliferation and mapped them to the comprehensive human interactome (24), which represents a network of all ascertainable protein-protein interactions in a cell. As a result, a miRNA regulatory network in COPD describing the dysfunctional cell proliferation module was constructed (Figure 2).

Correlation of miRNA expression with COPD severity and vascular remodeling

Among the differentially expressed miRNAs, the expression levels of miR-139 and miR-485 correlated with the severity of airflow obstruction, assessed by the percent predicted value of

the forced expiratory volume in the first second (FEV₁) (Figure E3). The expression of miR-197 was significantly correlated with the severity of airflow obstruction (the lower the miRNA expression, the lower the FEV₁) and inversely correlated to the vascular remodeling degree, assessed by the thickness of the intimal layer (the lower the miRNA expression, the greater the intimal thickness) (Figure 3A). Expression of miR-98 and miR-451 also correlated with airflow obstruction and intimal thickness (Figure 3B and 3C).

Expression of miR-197 increases during SMC differentiation

Among all miRNAs that correlated with pulmonary function parameters, the contribution of miR-197 was consistent and had not been previously evaluated in processes involving vascular remodeling. miR-197 function has been associated with the regulation of cell cycle related genes and has been shown to modulate SMC proliferation in leiomyoma (25, 26). Using an *in vitro* model of SMC differentiation induced by cell-to-cell contact (4), we performed Northern blot analysis at different stages of differentiation –D0 (proliferative cells), D2 (confluent cells), and D6 (differentiated/contractile cells)– and observed that miR-197 expression was increased in differentiated SMC with contractile phenotype (Figure 4A).

In SMC isolated from pulmonary arteries of the studied subjects, Northern blot analysis showed reduced expression of miR-197 in SMC from COPD patients and SK, as compared to NS (Figure 4B).

Effect of miR-197 inhibition on SMC differentiation and proliferation

Transfection of SMC with a 2'-O-methylated antisense RNA against miR-197 (AS-miR-197) and a scrambled AS (AS-miR-CTL) at D0 of differentiation was used to inhibit the expression of miR-197 (Figure 5A). MiR-197 inhibition in SMC blunted the expression of the

SMC differentiation markers, myocardin, calponin, and sm22- α , after induction of differentiation by cell-to-cell contact (22) as assessed by RT-qPCR (Figure 5B). Analysis of both α -SMA and calponin by immunofluorescence showed a marked decrease of actin and calponin fiber formation in AS-miR-197-transfected cells as compared with control cells (Figure 5B). In addition, miR-197 inhibition induced the proliferation of SMC as measured by increased expression of Ki67 at RNA and protein levels (Figure 5C). In agreement with these results, proliferation and migration capacities analyzed by a wound-healing assay were significantly increased in SMC after transfection with AS-miR-197 (Figure 5D).

MiR-197 targets the transcription factor E2F1

Co-transfection of E2F1 3'UTR coupled to a luciferase report vector with the AS-miR-197 in SMC (Figure 6A) showed increased luciferase expression compared to cells that received the scrambled control miRNA inhibitor. In addition, upregulation of E2F1 RNA was observed after miR-197 inhibition in differentiated SMC (Figure 6B). These results confirm that miR-197 targets mRNA encoding the transcription factor E2F1. According to these results, E2F1 expression followed an inverse pattern as that of miR-197 during SMC differentiation (Figure 6C).

Expression of E2F1 is increased in PA from COPD patients

Representative microphotographs of immunohistochemical stains for both the endothelial marker CD31 (Figure 7A) and smooth muscle- α actin (Figure 7B) of pulmonary arteries used in this study are shown in Figure 7. Enlargement of the vessel wall is apparent in pulmonary arteries from COPD patients (Figure 7B). Such an enlargement is mainly due to the proliferation of smooth muscle α actin-expressing cells (Figure 7B).

To investigate whether or not the expression of E2F1 might be dysregulated in pulmonary arteries from COPD patients, we analyzed the expression of E2F1 by immunohistochemistry (Figures 7D and 7E) and Western Blot (Figure 7F). The expression of E2F1 in the COPD and the SK groups was upregulated, as compared with the NS, mirroring the downregulation of miR-197 in COPD pulmonary arteries.

DISCUSSION

The present study demonstrates the involvement of miRNAs in COPD-related vascular remodeling. Our work shows that from the 381 studied miRNAs, only 2% of miRNAs were differentially expressed in pulmonary arteries of COPD patients compared to NS. By applying Limma analysis, we identified 8 deregulated miRNAs in COPD. From these miRNAs, miR-98, miR-139-5p, miR-146b-5p, and miR-451 were upregulated, and miR-197, miR-204, miR-485-3p, and miR-627 were downregulated. Interestingly, expression of miRNAs in pulmonary arteries from SK was similar to that of COPD patients, although they did not achieve significance, indicating that smoking without airflow obstruction is an intermediate phenotype between NS and COPD, as has been already suggested in other studies (27, 28).

The gene ontology (GO) annotation analysis of all of these miRNAs using the TargetScan database identified mainly genes involved in cell proliferation, suggesting that vascular remodeling in COPD is associated with changes in miRNAs that control cell proliferation. By mapping these targets, we constructed a miRNA regulatory network, which represents a cell proliferation functional module in COPD as compared to NS. This approach allowed us to identify the miRNAs and their canonical targets associated with multiple pathogenic pathways central to SMC proliferation in COPD.

We documented a downregulation of miR-204 in PA of COPD patients. In addition, a decreased expression of miR-204 was observed in both proliferative SMC and in SMC pulmonary arteries-derived SMC from COPD patients (Figure E4). In support of this finding, reduced expression of miR-204 in SMC from pulmonary arteries in both PAH patients and in rodent experimental models of PAH have been reported (14). Downregulation of miR-204 in dedifferentiated SMC suggests that miR-204 has a potential role in regulating SMC differentiation. Interestingly, miR-204 targets the transcription factor Slug in cancer cells, regulating changes in cell phenotype (29, 30). In this regard, we have recently shown that Slug modulates the SMC proliferative phenotype, and that its expression is increased in both highly remodeled human PA and in lungs of mice with severe PH (22). These results indicate that miR-204 might regulate SMC phenotype through suppressing Slug expression as has been previously suggested (16).

In pulmonary arteries of COPD patients, we also observed upregulation of miR-451, as has been shown in experimental models of PH and in humans with PAH (11). The transient loss of miR-451 is protective in the development of PAH (34). Other dysregulated miRNA in this study were miR-146b, which is known to promote SMC proliferation (31) and miR-98, which mediates endothelial inflammation in atherosclerosis (32). Finally, miR-197, miR-485, and miR-627 are broadly involved in cancer cell proliferation (33, 31, 33, 26). We hypothesized that deregulation of miRNAs might promote cell proliferation and contribute to intimal hyperplasia in pulmonary arteries in COPD.

Among dysregulated miRNAs, the degree of vascular remodeling and the severity of airflow obstruction were associated to the upregulation of both miR-98 and miR-451, and the downregulation of miR-197. The miRNA that displayed both the strongest correlation and the highest consistency in relation to parameters of disease severity was miR-197. Interestingly,

miR-197 has been found to be downregulated in leiomyoma, promoting SMC proliferation (26, 34), and eventually it might also be involved in SMC proliferation in other disorders. Accordingly, we further analyzed the role of miR-197 in modulating the proliferative phenotype of PA SMC using an *in vitro* model of SMC differentiation. Our results show that an increased expression of miR-197 was associated with a SMC differentiated/contractile phenotype, whereas its inhibition downregulated mature markers of SMC in differentiated cells. Moreover, functional studies performed after transfection of SMC with the AS-miR-197 revealed that this miRNA regulates SMC phenotype denoted by higher rates of proliferation/migration. Cultured SMC obtained from explanted PA of COPD patients also showed low levels of miR-197 that was associated with a less differentiated phenotype.

Available data indicate that miRNA-197 binds to the 3'-untranslated region (3'-UTR) of E2F1 (35). This is important because E2F1 is an oncoprotein that regulates many cellular processes, including cell proliferation (36). E2F1 participates in both cell cycle progression and apoptosis, depending on which pathway is activated (37, 38). E2F1 induces S phase entry, activating prosurvival and proliferative genes like cyclins, p53, or c-myc, and many S-phase genes (39, 40), whereas activation of the regulators p53, p73, or Bcl2 induces apoptosis. In our study with PA SMC, using a luciferase report assay and qPCR, we validated that E2F1 is a target of miR-197. E2F1 expression was high in proliferative/dedifferentiated SMC in accordance with oncogene function, and decreased during the acquisition of a contractile phenotype, following an inverse pattern than that of miR-197 expression. Importantly, we found that E2F1 was upregulated, paralleling the decreased expression of miR-197, in PA from COPD patients. The localization of E2F1 protein in remodeled arteries corresponds to sites of SMC proliferation in the vessel wall. These results agree with previous studies showing that E2F1 and its targets regulate SMC proliferation and vessel remodeling

(41, 42). In addition, E2F1 is expressed in the endothelium. Further studies are needed to analyze which cell population in the enlarged artery wall contribute to the downregulation of miR-197. Our results indicate that SMC derived from smokers and COPD patients exhibit decreased miR-197 expression. As miR-197 is also expressed in EC, future studies should analyze the expression of this miRNA in endothelial cells derived from COPD patients.

By using network analysis, we documented that miR-197 binds canonically with at least 19 different factors related to cell proliferation. From these factors we confirmed the increased expression of insulin growth factor-1 (IGF1) after miR-197 inhibition (Figure E4), a known factor involved in both pulmonary vascular remodeling (43) and stimulation of SMC proliferation (44). This result suggests that IGF-1 might also be a target of miR-197, but more studies are needed in order to validate it.

Further studies are needed to unravel the mechanisms by which miR-197 is downregulated in COPD-associated vascular remodeling. Cigarette smoke products might alter miR-197 expression. Nicotine induces STAT3 activation in both smooth muscle and inflammatory cells (45). STAT3 promotes the downregulation of miR-204 in SMC by epigenetic mechanisms (46). Interestingly, in hepatocellular carcinoma cells, activation of the interleukin-6 (IL-6)/STAT3 pathway induces the downregulation of miR-197, which, in turn, targets stat3 mRNA to promote cancer progression (31). However, smoking, as an intermediate condition (30), is not enough to explain COPD alteration. Hypoxia might also promote miR-197 downregulation. In this respect, IL-6 is increased in cells with both a hypoxic environment and a more proliferative/dedifferentiated SMC phenotype in pulmonary hypertension (47). The mechanism of miRNA-197 downregulation might also involve DNA hypermethylation, which is known to induce the downregulation of tumor suppressor miRNAs in cancer (48) and has also been described in vascular remodeling (46).

The present study has some limitations. First, despite the fact that pulmonary arteries were isolated in an area distant from the solid tumor, we cannot exclude some effects of tumor factors on miRNA expression. Considering this, we performed an additional network analysis discriminating different cancer types, specifically squamous vs. non-squamous cancers. In this analysis, miR-197 did not show any difference among cancer samples (data not shown). Second, due to the difficulties in obtaining adequate lung tissue from COPD patients and control subjects, the small sample size represents another limitation of this study. Third, we were unable to correlate the documented miRNA profile with the status of SMC differentiation *in vivo* at the moment of miRNA analysis, due to limitations in obtaining good quality and adequate quantity of PA tissue and the impossibility to *in vivo* cell-track the SMC lineage.

In summary, we observed downregulation of miR-197 in pulmonary arteries from smokers and COPD patients. The expression of this miRNA was inversely related to the degree of vascular remodeling and the severity of airflow obstruction. E2F1, a transcription factor targeted by miR-197 was upregulated in pulmonary arteries from smokers and COPD patients. Taken together, our studies support the view that miR-197 downregulation induces a SMC proliferative phenotype, at least in part, by releasing the suppression of the E2F1 transcription factor, which, in turn, regulates cell cycle entry. Accordingly, miR-197, should be considered a contributing player among other dysregulated miRNAs in this condition. The combination of genes expression dysregulation leads to dysfunctional SMC in COPD promoting the “vascular remodeling phenotype” (49). The identification of miRNAs involved in cell proliferation associated with pulmonary vascular remodeling in COPD opens a new view in its pathogenesis and, eventually, its therapeutic approach.

Acknowledgments

This work was developed at the Centre de Recerca Biomèdica Cellex, Barcelona, Spain. We are indebted to the Citomics core facility of the Institut d'Investigacions Biomèdiques August Pi i Sunyer (IDIBAPS) for their technical help. We thank Cristina Bonjoch Anguita for expert technical assistance.

References

1. Peinado VI, Ramírez J, Roca J, Rodriguez-Roisin R, Barberà JA. Identification of vascular progenitor cells in pulmonary arteries of patients with chronic obstructive pulmonary disease. *Am J Respir Cell Mol Biol*. 2006 Mar;34(3):257–63.
2. Blanco I, Piccari L, Barberà JA. Pulmonary vasculature in COPD: The silent component. *Respirol Carlton Vic*. 2016 Aug;21(6):984–94.
3. Santos S, Peinado VI, Ramírez J, Melgosa T, Roca J, Rodriguez-Roisin R, et al. Characterization of pulmonary vascular remodelling in smokers and patients with mild COPD. *Eur Respir J*. 2002 Apr;19(4):632–8.
4. Coll-Bonfill N, de la Cruz-Thea B, Pisano MV, Musri MM. Noncoding RNAs in smooth muscle cell homeostasis: implications in phenotypic switch and vascular disorders. *Pflugers Arch*. 2016;468(6):1071–1087.
5. Barberà JA, Peinado VI. Vascular progenitor cells in chronic obstructive pulmonary disease. *Proc Am Thorac Soc*. 2011 Nov;8(6):528–34.
6. Stenmark KR, Davie N, Frid M, Gerasimovskaya E, Das M. Role of the adventitia in pulmonary vascular remodeling. *Physiol Bethesda Md*. 2006 Apr;21:134–45.
7. Bartel DP. MicroRNAs: genomics, biogenesis, mechanism, and function. *Cell*. 2004 Jan 23;116(2):281–97.
8. Meister G, Landthaler M, Dorsett Y, Tuschl T. Sequence-specific inhibition of microRNA- and siRNA-induced RNA silencing. *RNA*. 2004;10(3):544–550.
9. McDonald RA, Hata A, MacLean MR, Morrell NW, Baker AH. MicroRNA and vascular remodelling in acute vascular injury and pulmonary vascular remodelling. *Cardiovasc Res*. 2012 Mar 15;93(4):594–604.
10. Nazari-Jahantigh M, Wei Y, Schober A. The role of microRNAs in arterial remodelling. *Thromb Haemost*. 2012 Apr;107(4):611–8.
11. Leopold JA, Maron BA. Molecular Mechanisms of Pulmonary Vascular Remodeling in Pulmonary Arterial Hypertension. *Int J Mol Sci* [Internet]. 2016;17(5). Available from: <http://www.ncbi.nlm.nih.gov/pubmed/27213345>
12. Bockmeyer CL, Maegel L, Janciauskiene S, Rische J, Lehmann U, Maus UA, et al. Plexiform vasculopathy of severe pulmonary arterial hypertension and microRNA expression. *J Heart Lung Transplant Off Publ Int Soc Heart Transplant*. 2012 Jul;31(7):764–72.
13. Cheng Y, Liu X, Yang J, Lin Y, Xu D-Z, Lu Q, et al. MicroRNA-145, a novel smooth muscle cell phenotypic marker and modulator, controls vascular neointimal lesion formation. *Circ Res*. 2009 Jul 17;105(2):158–66.

14. Courboulin A, Paulin R, Giguère NJ, Saksouk N, Perreault T, Meloche J, et al. Role for miR-204 in human pulmonary arterial hypertension. *J Exp Med*. 2011 Mar 14;208(3):535–48.
15. Lee Y, Kim M, Han J, Yeom K-H, Lee S, Baek SH, et al. MicroRNA genes are transcribed by RNA polymerase II. *EMBO J*. 2004 Oct 13;23(20):4051–60.
16. Zhou G, Chen T, Usha Raj J. MicroRNAs in pulmonary arterial hypertension. *Am J Respir Cell Mol Biol*. 2015;52(2):139–151.
17. Pullamsetti SS, Doebele C, Fischer A, Savai R, Kojonazarov B, Dahal BK, et al. Inhibition of microRNA-17 improves lung and heart function in experimental pulmonary hypertension. *Am J Respir Crit Care Med*. 2012 Feb 15;185(4):409–19.
18. Davis-Dusenbery BN, Chan MC, Reno KE, Weisman AS, Layne MD, Lagna G, et al. down-regulation of Kruppel-like factor-4 (KLF4) by microRNA-143/145 is critical for modulation of vascular smooth muscle cell phenotype by transforming growth factor-beta and bone morphogenetic protein 4. *J Biol Chem*. 2011 Aug 12;286(32):28097–110.
19. Izzotti A, Calin GA, Steele VE, Croce CM, De Flora S. Relationships of microRNA expression in mouse lung with age and exposure to cigarette smoke and light. *FASEB J Off Publ Fed Am Soc Exp Biol*. 2009 Sep;23(9):3243–50.
20. Schembri F, Sridhar S, Perdomo C, Gustafson AM, Zhang X, Ergun A, et al. MicroRNAs as modulators of smoking-induced gene expression changes in human airway epithelium. *Proc Natl Acad Sci U S A*. 2009 Feb 17;106(7):2319–24.
21. Kara M, Kirkil G, Kalemci S. Differential Expression of MicroRNAs in Chronic Obstructive Pulmonary Disease. *Adv Clin Exp Med Off Organ Wroclaw Med Univ*. 2016 Feb;25(1):21–6.
22. Coll-Bonfill N, Peinado VI, Pisano MV, Párrizas M, Blanco I, Evers M, et al. Correction: Slug is increased in vascular remodeling and induces a smooth muscle cell proliferative phenotype (PLoS ONE (2016) 11:7 (e0159460) DOI: 10.1371/journal.pone.0159460). *PLoS ONE*. 2016;11(8).
23. Diez Musri, M. M. M, Ferrer E, Barbera JA, Peinado VI. Endothelial progenitor cells undergo an endothelial-to-mesenchymal transition-like process mediated by TGFbetaRI. *Cardiovasc Res*. 2010;88(3):502–511.
24. Menche J, Sharma A, Kitsak M, Ghiassian SD, Vidal M, Loscalzo J, et al. Disease networks. Uncovering disease-disease relationships through the incomplete interactome. *Science*. 2015 Feb 20;347(6224):1257601.
25. Tian L-Q, Liu E-Q, Zhu X-D, Wang X-G, Li J, Xu G-M. MicroRNA-197 inhibits cell proliferation by targeting GAB2 in glioblastoma. *Mol Med Rep*. 2016 May;13(5):4279–88.
26. Ling J, Jiang L, Zhang C, Dai J, Wu Q, Tan J. Upregulation of miR-197 inhibits cell proliferation by directly targeting IGFBP5 in human uterine leiomyoma cells. *In Vitro Cell Dev Biol Anim*. 2015 Sep;51(8):835–42.

27. Peinado VI, Barberá JA, Abate P, Ramírez J, Roca J, Santos S, et al. Inflammatory reaction in pulmonary muscular arteries of patients with mild chronic obstructive pulmonary disease. *Am J Respir Crit Care Med*. 1999 May;159(5 Pt 1):1605–11.
28. Llinàs L, Peinado VI, Ramon Goñi J, Rabinovich R, Pizarro S, Rodriguez-Roisin R, et al. Similar gene expression profiles in smokers and patients with moderate COPD. *Pulm Pharmacol Ther*. 2011 Feb;24(1):32–41.
29. Qiu YH, Wei YP, Shen NJ, Wang ZC, Kan T, Yu WL, et al. miR-204 inhibits epithelial to mesenchymal transition by targeting slug in intrahepatic cholangiocarcinoma cells. *Cell Physiol Biochem*. 2013;32(5):1331–1341.
30. Yu C-C, Chen P-N, Peng C-Y, Yu C-H, Chou M-Y. Suppression of miR-204 enables oral squamous cell carcinomas to promote cancer stemness, EMT traits, and lymph node metastasis. *Oncotarget*. 2016 Apr 12;7(15):20180–92.
31. Wang H, Su X, Yang M, Chen T, Hou J, Li N, et al. Reciprocal control of miR-197 and IL-6/STAT3 pathway reveals miR-197 as potential therapeutic target for hepatocellular carcinoma. *Oncoimmunology*. 2015 Oct;4(10):e1031440.
32. Chen L-J, Chuang L, Huang Y-H, Zhou J, Lim SH, Lee C-I, et al. MicroRNA mediation of endothelial inflammatory response to smooth muscle cells and its inhibition by atheroprotective shear stress. *Circ Res*. 2015 Mar 27;116(7):1157–69.
33. Formosa A, Markert EK, Lena AM, Italiano D, Finazzi-Agro' E, Levine AJ, et al. MicroRNAs, miR-154, miR-299-5p, miR-376a, miR-376c, miR-377, miR-381, miR-487b, miR-485-3p, miR-495 and miR-654-3p, mapped to the 14q32.31 locus, regulate proliferation, apoptosis, migration and invasion in metastatic prostate cancer cells. *Oncogene*. 2014 Oct 30;33(44):5173–82.
34. Xin J, Zhang X-K, Xin D-Y, Li X-F, Sun D-K, Ma Y-Y, et al. FUS1 acts as a tumor-suppressor gene by upregulating miR-197 in human glioblastoma. *Oncol Rep*. 2015 Aug;34(2):868–76.
35. Helwak A, Kudla G, Dudnakova T, Tollervey D. Mapping the human miRNA interactome by CLASH reveals frequent noncanonical binding. *Cell*. 2013 Apr 25;153(3):654–65.
36. Attwooll C, Lazzerini Denchi E, Helin K. The E2F family: specific functions and overlapping interests. *EMBO J*. 2004 Dec 8;23(24):4709–16.
37. Crosby ME, Almasan A. Opposing roles of E2Fs in cell proliferation and death. *Cancer Biol Ther*. 2004 Dec;3(12):1208–11.
38. DeGregori J, Johnson DG. Distinct and Overlapping Roles for E2F Family Members in Transcription, Proliferation and Apoptosis. *Curr Mol Med*. 2006 Nov;6(7):739–48.
39. Helin K. Regulation of cell proliferation by the E2F transcription factors. *Curr Opin Genet Dev*. 1998 Feb;8(1):28–35.

40. Yan H, Xue G, Mei Q, Wang Y, Ding F, Liu M-F, et al. Repression of the miR-17-92 cluster by p53 has an important function in hypoxia-induced apoptosis. *EMBO J*. 2009 Sep 16;28(18):2719–32.
41. Dapas B, Farra R, Grassi M, Giansante C, Fiotti N, Uxa L, et al. Role of E2F1-cyclin E1-cyclin E2 circuit in human coronary smooth muscle cell proliferation and therapeutic potential of its downregulation by siRNAs. *Mol Med Camb Mass*. 2009 Oct;15(9–10):297–306.
42. Endorf EB, Qing H, Aono J, Terami N, Doyon G, Hyzny E, et al. Telomerase Reverse Transcriptase Deficiency Prevents Neointima Formation Through Chromatin Silencing of E2F1 Target Genes. *Arterioscler Thromb Vasc Biol*. 2017 Feb;37(2):301–11.
43. Perkett EA, Badesch DB, Roessler MK, Stenmark KR, Meyrick B. Insulin-like growth factor I and pulmonary hypertension induced by continuous air embolization in sheep. *Am J Respir Cell Mol Biol*. 1992 Jan;6(1):82–7.
44. von der Thüsen JH, Borensztajn KS, Moimas S, van Heiningen S, Teeling P, van Berkel TJC, et al. IGF-1 has plaque-stabilizing effects in atherosclerosis by altering vascular smooth muscle cell phenotype. *Am J Pathol*. 2011 Feb;178(2):924–34.
45. Li J-M, Cui T-X, Shiuchi T, Liu H-W, Min L-J, Okumura M, et al. Nicotine enhances angiotensin II-induced mitogenic response in vascular smooth muscle cells and fibroblasts. *Arterioscler Thromb Vasc Biol*. 2004 Jan;24(1):80–4.
46. Kim J-D, Lee A, Choi J, Park Y, Kang H, Chang W, et al. Epigenetic modulation as a therapeutic approach for pulmonary arterial hypertension. *Exp Mol Med*. 2015;47:e175.
47. Frid MG, Li M, Gnanasekharan M, Burke DL, Fragoso M, Strassheim D, et al. Sustained hypoxia leads to the emergence of cells with enhanced growth, migratory, and promitogenic potentials within the distal pulmonary artery wall. *Am J Physiol Lung Cell Mol Physiol*. 2009 Dec;297(6):L1059-1072.
48. Lujambio A, Calin GA, Villanueva A, Ropero S, Sánchez-Céspedes M, Blanco D, et al. A microRNA DNA methylation signature for human cancer metastasis. *Proc Natl Acad Sci U S A*. 2008 Sep 9;105(36):13556–61.
49. Pullamsetti SS, Perros F, Chelladurai P, Yuan J, Stenmark K. Transcription factors, transcriptional coregulators, and epigenetic modulation in the control of pulmonary vascular cell phenotype: therapeutic implications for pulmonary hypertension (2015 Grover Conference series). *Pulm Circ*. 2016 Dec;6(4):448–64.

Figure Legends

Table 1. Characteristics of the patients enrolled in this study. * $p < 0.05$ NS vs COPD, † $p < 0.05$ S vs COPD and ‡ $p < 0.05$ NS vs SK. COPD, chronic obstructive pulmonary disease; SK, smokers; NS, non-smokers.

Table 2. miRNA expression in COPD patients. Table showing the dysregulated miRNAs in PA from COPD, SK and NS. FC, fold change; COPD, chronic obstructive pulmonary disease; SK, smokers; NS, non-smokers.

Figure 1. miRNA expression in COPD patients. Graphic representing the fold change of the top 8 deregulated miRNAs. * $p < 0.05$. FC, fold change; COPD, chronic obstructive pulmonary disease; SK, smokers; NS, non-smokers.

Figure 2. A miRNA regulatory network in COPD. The green nodes represent miRNAs, and the blue nodes are miRNA targets. All the target genes have the annotation 'cell proliferation'.

Figure 3. Correlation analysis of miRNA expression with both FEV1 and intimal enlargement. **A**, Negative correlation between miR-197 expression (ddCt) and FEV1 * $p < 0.05$ by Pearson (left panel). Positive correlation between miR-197 expression (ddCt) and % intima respect to total area * $p < 0.05$ by Spearman analysis (right panel). **B**, Positive correlation between miR-451 expression (ddCt) and FEV1 * $p < 0.05$ by Pearson (left panel) and Negative correlation between miR-451 expression (ddCt) and % intima respect to total area * $p < 0.05$ by Spearman (right panel). **C**, Positive

correlation between miR-98 expression (ddCt) and FEV1 * $p < 0.05$ by Pearson (left panel) and Negative correlation between miR-98 expression (ddCt) and % intima respect to total area * $p < 0.05$ by Spearman (right panel).

Figure 4. Analysis of miR-197 expression and SMC phenotypic change and in SMC from patients. **A**, Representative Northern Blot showing an increase of miR-197 in differentiated (D6) as compared to proliferative (D0) SMC cells. **B**, Representative Northern Blot showing the downregulation of miR-197 in SMC derived from PA of SK (n=3) and COPD patients (n=3) respect to control patients (n=3).

Figure 5. Inhibition of miR-197 abrogates SMC differentiation. **A**, Northern blot analysis of miR-197 after 48 hours of transfection with AS-miR-197 (antisense to miR-197) and a scrambled control (AS-miR-CT) in SMC. AS-miR-197 blunted the expression of miR-197 in SMC. **B**, Transfection of AS miR-197 induces a SMC phenotype switching as is shown by the concomitant decrease of the SMC markers myoCD, sm22- α , calponin analysed by real time PCR and by the decrease of actin and calponin fibers assessed by immunofluorescence. **C**, miR-197 inhibition promoted an increase in the expression of the marker of proliferation Ki67 at both RNA (left panel) and protein levels (right panel). **D**, Scratch analysis shows an increased migration rate of SMC transfected with AS-miR-197 respect to the scrambled control correlating well with SMC dedifferentiation. * $p < 0.05$ by paired-test. All experiments were performed at least 3 times in duplicate.

Figure 6. The transcription factor E2F1 is a target of miR-197. **A**, Luciferase assay shows an increase in luciferase units after miR-197 inhibition corroborating that E2F1 is

a miR-197 target. **B**, E2F1 expression decreases along SMC differentiation performed by PCR **C**, miR-197 inhibition promotes the increase of E2F1 expression analysed by real time PCR. * $p < 0.05$ by paired-test. All experiments were performed at least 3 times in duplicate, except the luciferase assay that was performed 2 times in triplicates.

Figure 7. The transcription factor E2F1 is increased in PA from COPD patients.

Representative microphotographs of immunostaining of pulmonary artery sections from nonsmoker (n=3), smoker (n=5) and COPD patients (n=6) (A) CD31 (B) and smooth muscle alpha-actin immunohistochemistry of pulmonary arteries showing increased expression of alpha-actin in the media and intima of COPD patients. E2F1 immunohistochemistry (C and D) and immunodetection (E) in pulmonary arteries displays an increase in COPD and SK patients as compared to controls. $p < 0.05$ by one way ANOVA.

Table 1. Characteristics of the population.

	Non-Smokers	Smokers	COPD
	(n=7)	(n=9)	(n=12)
Age	63 ± 11	64 ± 10	67 ± 9
Male Gender, n (%)	4 (50)	8 (88) ‡	13 (100) *
Weight (kg)	64 ± 7	73 ± 8	70 ± 8
Height (cm)	161 ± 8	164 ± 8	169 ± 5
BMI	25 ± 3	28 ± 4	25 ± 2
FEV₁ (% predicted)	100 ± 6	90 ± 22	64 ± 13 * †
FVC (% predicted)	96 ± 7	93 ± 12	84 ± 13 *
FEV₁/FVC (% predicted)	77 ± 7	70 ± 15	55 ± 8 * †
Smoking history (pack/year)	5 ± 8	59 ± 27 ‡	77 ± 29 *
DL_{CO} (% predicted)	89 ± 20	75 ± 31	66 ± 11 *
PaO₂ (mmHg)	88 ± 15	81 ± 14	79 ± 16

Table 2. miRNAs with altered expression in pulmonary arteries from patients

	COPD vs NS		COPD vs SK		SK vs NS	
	FC	p-Value	FC	p-Value	FC	p-Value
hsa-miR-485-3p	-3,38	0,0064	-1,35	0,2671	-2,50	0,0697
hsa-miR-197	-3,18	0,0117	-1,90	0,1095	-1,67	0,3271
hsa-miR-139-5p	1,95	0,0173	1,69	0,0353	2,06	0,0636
hsa-miR-146b-5p	2,84	0,0178	2,73	0,0015	1,51	0,2000
hsa-miR-451	5,27	0,0263	1,63	0,4802	3,24	0,1967
hsa-miR-627	-2,27	0,0382	-1,27	0,3910	-1,79	0,1946
hsa-miR-204	-1,70	0,0385	1,05	0,8668	-1,78	0,1376
hsa-miR-98	2,37	0,0413	1,81	0,0851	1,31	0,2600

miRNA expression

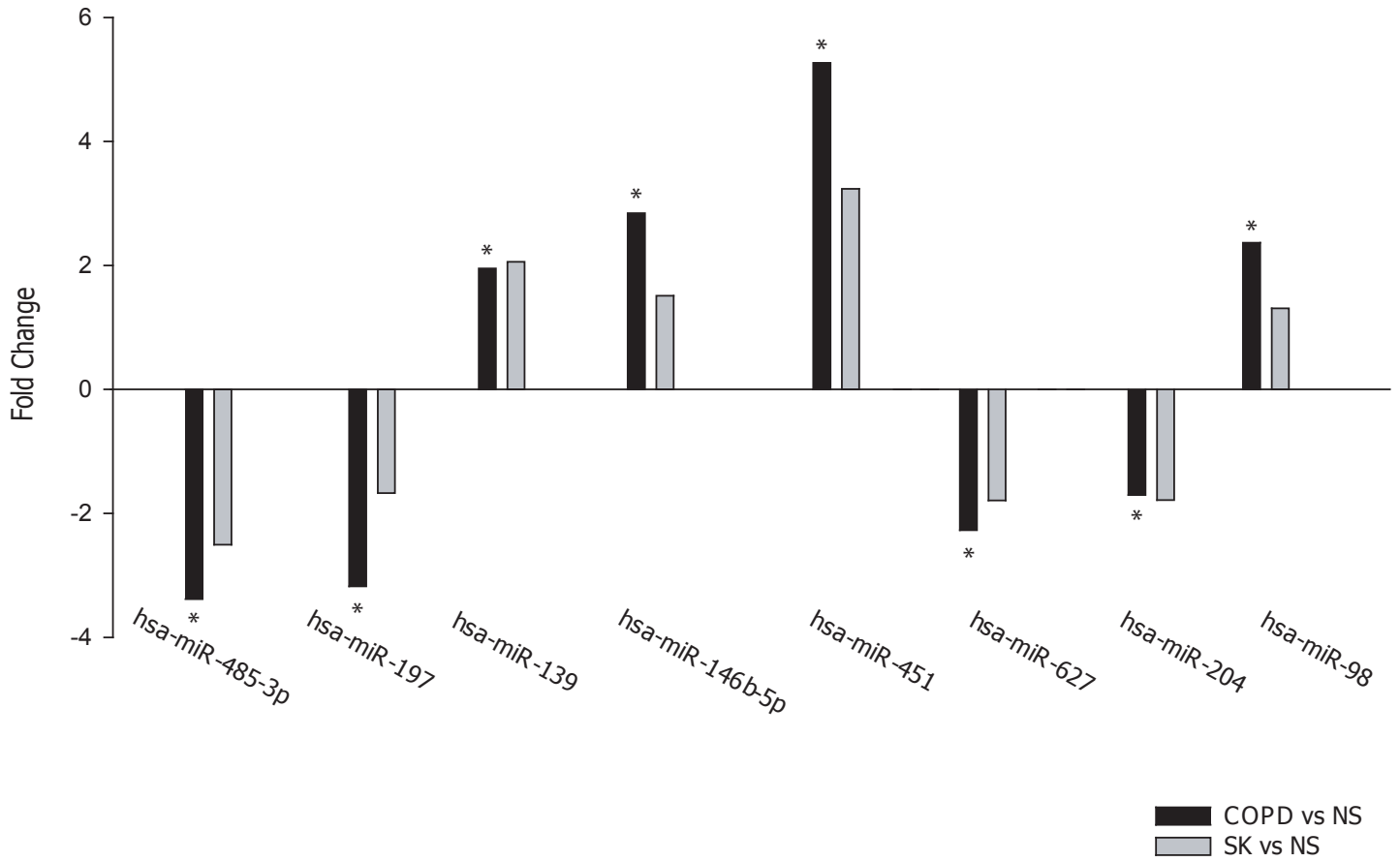


Figure 1

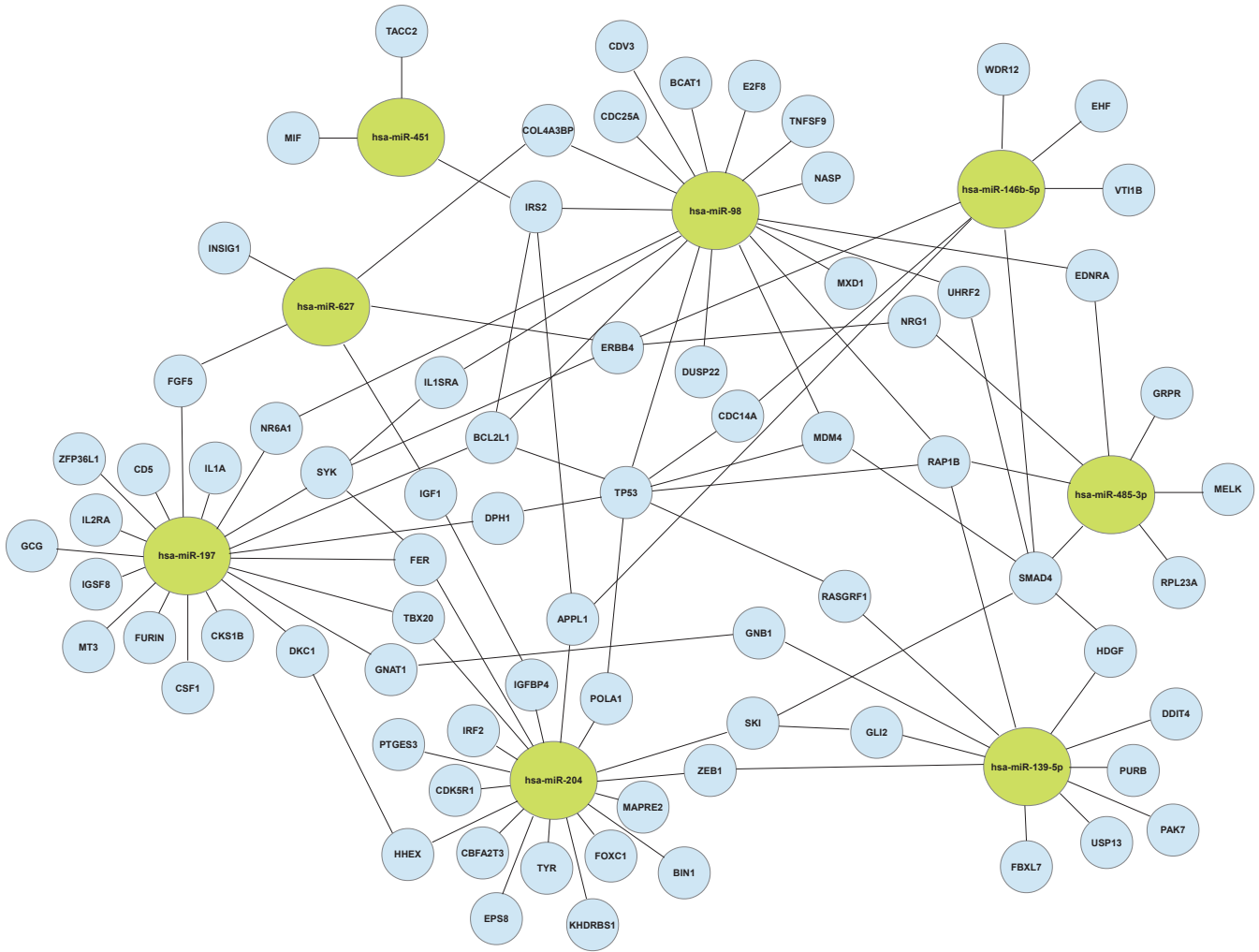


Figure 2

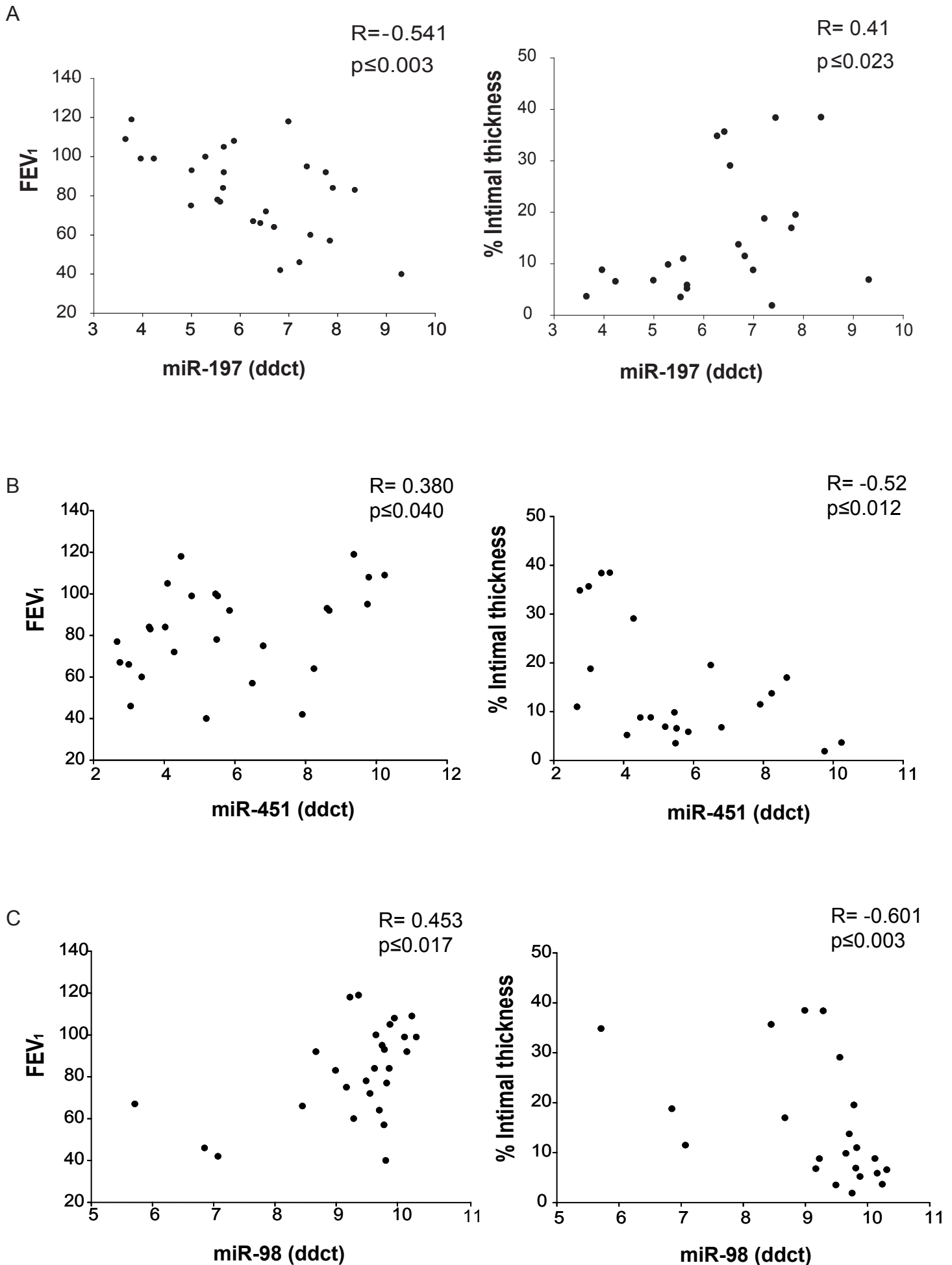


Figure 3

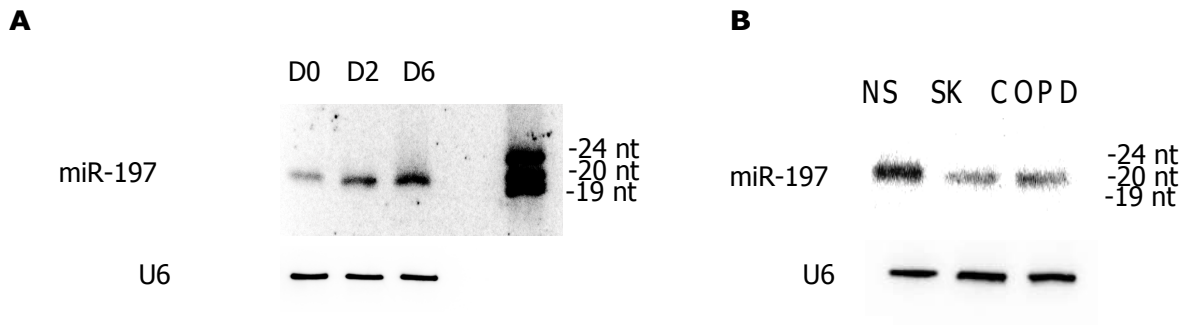
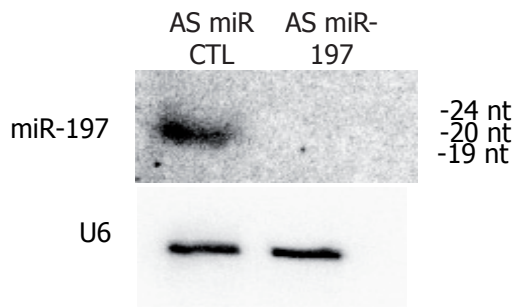
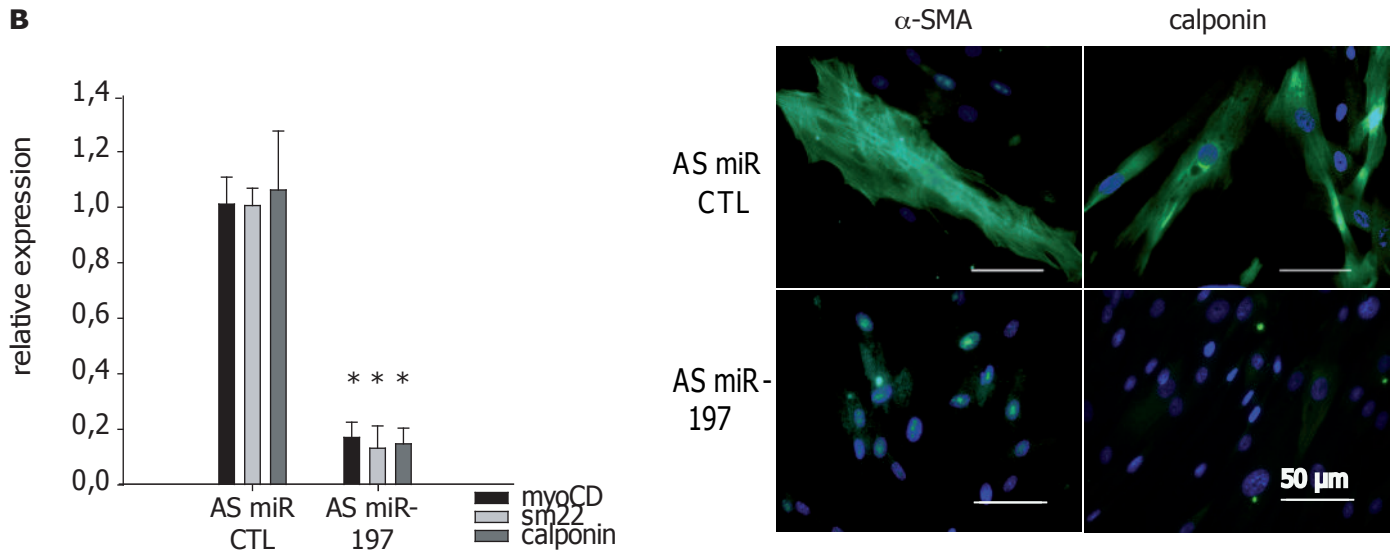
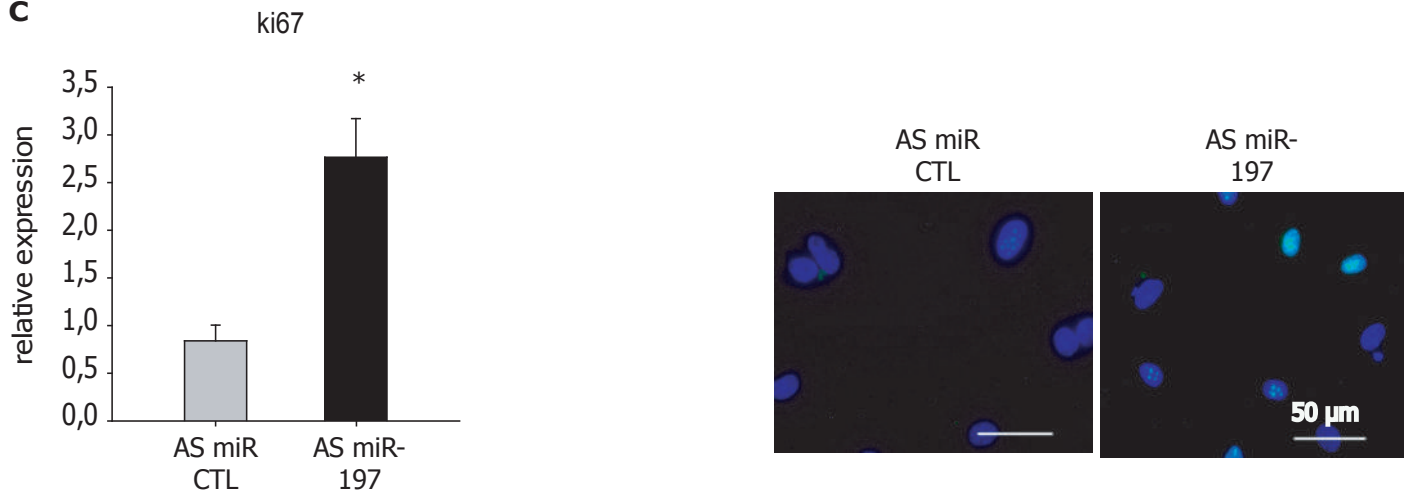
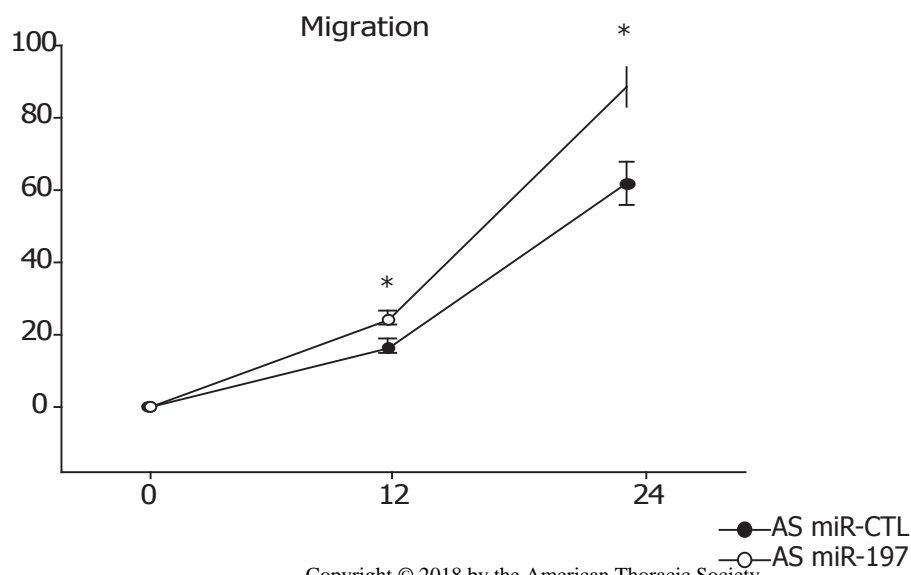


Figure 4

A**B****C****D****Figure 5**

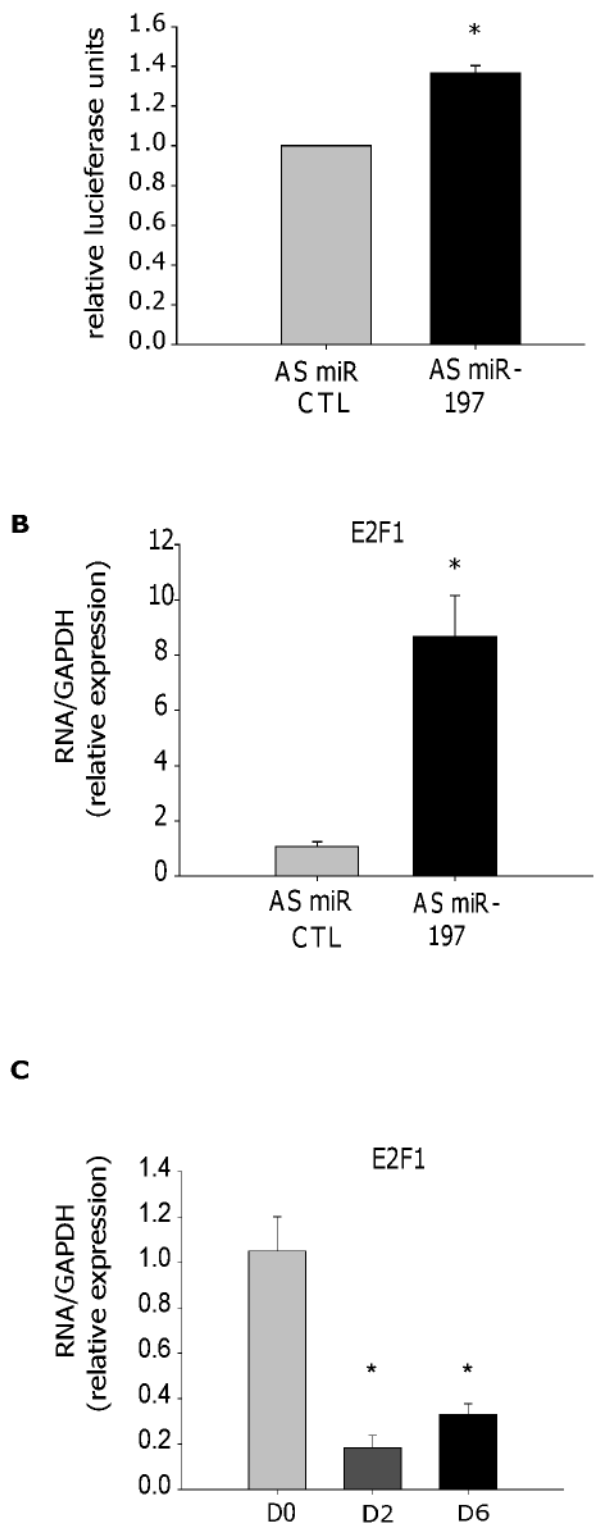


Figure 6

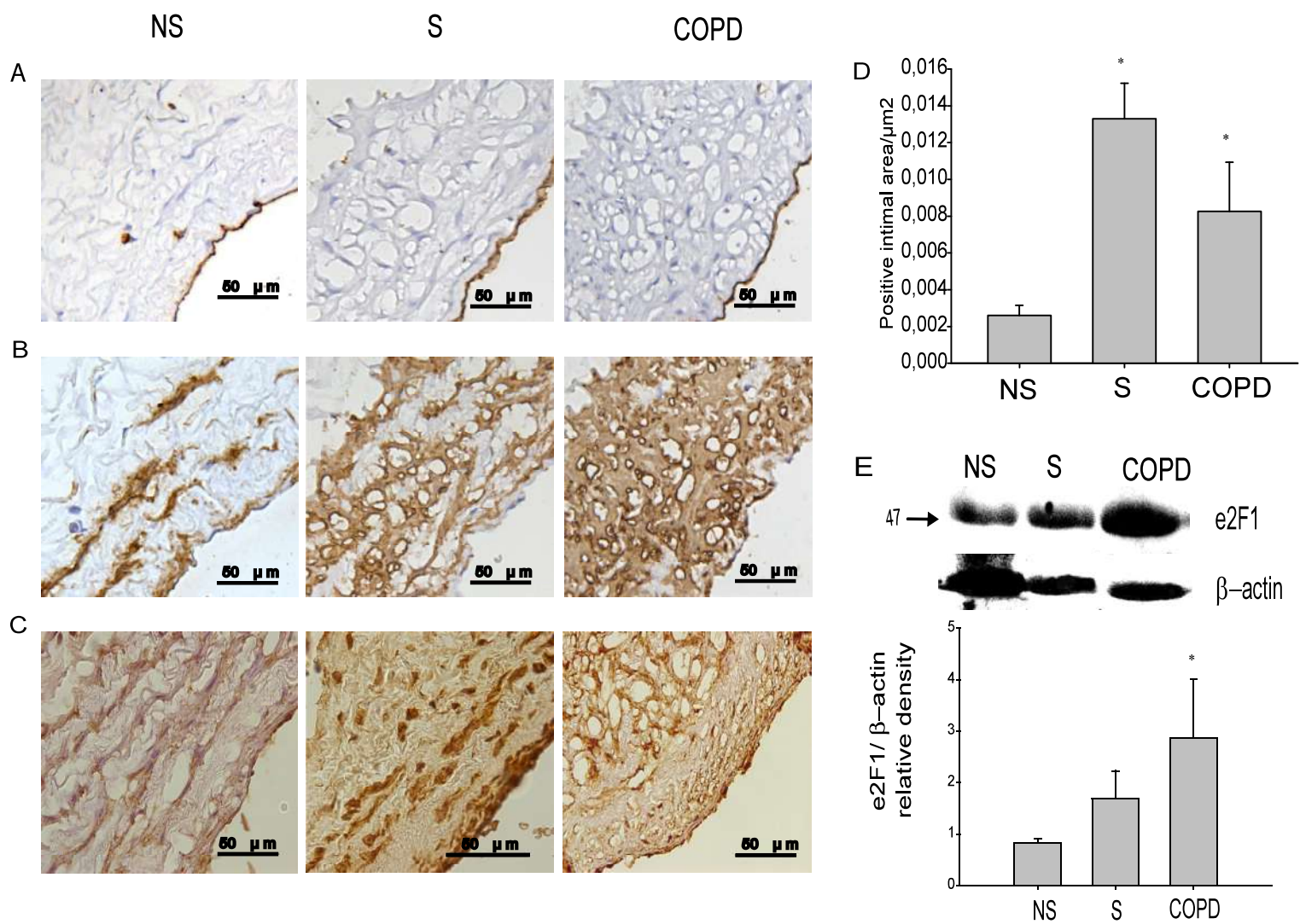


Figure 7

SUPPLEMENTARY DETAILED METHODS

Pulmonary arteries isolation

Pulmonary arteries measuring approximately 2 cm long with an external diameter of 1–2 mm were dissected under microscope and cleaned of surrounding parenchyma and connective tissue. Segments were preserved in RNAlater® solution (Ambion, Grand Island, NY) and frozen at -20°C until RNA extraction using TRIzol® Reagent (Invitrogen, Grand island, NY). RNA quality was checked with the LabChip® Test kit using the Agilent 2100 bioanalyzer (Agilent Technologies, Santa Clara, CA). Arterial wall morphometry was analyzed in cross-sectional rings of pulmonary arteries after elastic orcein staining, as previously described ²⁶. The area of the intimal layer was expressed as a percentage of the cross sectional area of the pulmonary artery.

SMC isolation from human PA

Cleaned pulmonary artery segments approximately 2 centimeters in length were obtained from NS, SK and COPD patients. They were cut in small pieces and seeded in a small flask with SmBM medium until SMC cells spread and migrated. Cells were passaged before they reached confluence, and passages between 4 and 8 were used. Primary cells obtained were characterized by the expression of SMC marker genes as α -actin and calponin by immunofluorescence at the D6 stage and by qPCR of mature markers during differentiation.

miRNA expression from pulmonary arteries

After RNA isolation, retrotranscription was performed using 10 ng of total RNA using the Taqman© miRNA reverse transcription kit and megaplex™ pools RT primers (Applied Biosystems) according to the manufacturers instructions. Taqman® array human miRNA cards A + B set v3.0 (Applied Biosystems)(TLDA) was used to analyze 381 miRNA expression.

miRNA differential expression and network analysis

An R/Bioconductor software package *limma* was used to identify differentially expressed miRNA in COPD vs. NS vs. SK, and COPD vs. SK.^{5,6} miRNAs with $p < 0.05$ and fold change > 1.5 were further analyzed. The target genes of these miRNAs were collected from TargetScanHuman 7.0.⁷ For those miRNAs that have targets with conserved sites, we considered all the targets, otherwise we only included the targets with a cumulative weighted context++ score ≥ 0.3 . The genes with annotation “cell proliferation” were obtained from the Gene Ontology (GO) database (www.geneontology.org/).⁸ We mapped the gene products of the targets with “cell proliferation” annotation to the human interactome⁹ and obtained an miRNA regulatory network in COPD v.s. NS.

Morphometric studies.

Pulmonary muscular arteries were analyzed in Formalin-fixed paraffin-embedded lung tissue sections processed with elastic orcein stain. All arteries with an external diameter < 1 mm and with complete elastic laminae were evaluated using an specific software for image-analysis (Leica-Qwin). Briefly, the external diameter was measured as the widest distance between external elastic laminae, perpendicular to the greatest longitudinal axis of each artery. External and internal elastic laminae and the inner aspect of the intima were outlined, and the area occupied by the muscular layer, the intimal layer, and the lumen was computed. Results were expressed as percentage of total area.

Primary cell culture

Human pulmonary artery smooth muscle cells (SMC) and human pulmonary artery endothelial cells (EC) were purchased from Lonza and cultured in SmBM and EgM-2 medium, respectively, supplemented with singleQuotsKitSuppl, growth factors (Lonza),

and 10% of fetal bovine serum (FBS) (Lonza). All cell lines were used at passages three to eight and maintained in a humidified atmosphere at 37°C in 5% CO₂.

Cell differentiation experiments

Briefly, SMC at 80% confluence were defined as dedifferentiated SMC (D0), cells at 100% confluence correspond to cells at the beginning of differentiation (D2), and SMC after 4 days of confluence were completely differentiated cells (D6). Total RNA was isolated using Trizol (Invitrogen) according to the manufacturer's instructions.

Functional Assays

Wound-healing assay

Forty thousand transfected cells were seeded in 48-well plates. After 48h of incubation, the culture was scratched with a sterile tip. Photomicrographs were taken at baseline and every 12h. The healing area was analyzed with Image-Pro Plus software (Media Cybernetics, Inc.)

miRNA inhibition

5 x 10⁴ SMC were seeded in 24-well plate and transfected with 40 nM 2' O-methyl antisense oligonucleotide to miR-197 chemically synthesized (Pierce) using Lipofectamine 2000 (Invitrogen). After indicated times, cells were harvested and RNA was isolated using TriZol (Invitrogen).

Luciferase assay

We used the modified pMIR-RL miRNA reporter plasmid with the E2F1 3'UTR and renilla luciferase as a transfection control as previously used (Ela Paper). Briefly, to generate the reporter plasmids, the pMIR-REPORT (Ambion) was modified as follows: The renilla luciferase gene with a SV40 promoter and a poly(A) site was PCR-amplified from the pRL-SV40 plasmid (Promega) and inserted into the SspI site of pMIR-REPORT. Additionally, an HSV-TK promoter was PCR-cloned from pRL-TK (Promega) and inserted into pMIR-REPORT to replace the CMV promoter of the firefly luciferase gene. Luciferase expression

construct was generated by cloning the 3'UTRs of E2F1 into the pMIR-RL described above. The 3'UTRs were cloned via PCR amplification from cDNA libraries and ligated into the corresponding SacI and NaeI sites of pMIR-RL. Primers used were: E2F1-Sac-for: 5'-CGCTACGCGTCAGGGTTGGAGGGACCAGGGT-3' and E2F1-NaeI-rev: 5'-CGCTGCCGGCAACGTCATCAAAATATTTATTA-3'. Plasmid transfections for luciferase assays were performed with 50 ng pMIR-RL-E2F1 3'UTR and 40 pmol 2'Ome-miR197-inhibitor (AS-miR-197) per 2×10^4 cells in a 48-well plate using lipofectamine 2000 (Invitrogen).

Expression analysis

RNA isolation and PCR detection

Total RNA was isolated using Trizol (Invitrogen) according to the manufacturer's instructions. Random-primed cDNA synthesis was performed at 37°C with 1 µg of RNA using the high capacity cDNA Kit (Applied Biosystems). Gene expression was measured by quantitative real time PCR in a Chromo 4 Real Time PCR detector (Bio-Rad, Hercules, CA USA) and ABI fast 7900 HT (Applied Biosystems) using the sensiMix dt kit (Quantace, San Mateo, CA, USA) based on the DNA double-strand-specific SYBR green I dye and Taqman© probes (Applied Biosystems) for detection. The results were normalized to *GAPDH* and *ACTB* expression levels and relative gene expression was analyzed by the 2-ddct method. The primer used and their sequences are listed in Table E2.

Western Blotting

SMC were washed with PBS and then lysed with RIPA buffer (50 mM TRIS-Cl, 150 mM NaCl, 1 mM EDTA, 10% NP-40, 0.10% deoxycholic acid) containing protease inhibitors (Sigma-Aldrich). The lysate was centrifuged at 14,000g for 15 min at 4°C to pellet debris, and the protein-rich supernatant was stored at -20°C. Total protein concentration

Online Figure Legends

Table E1. miRNA expression obtained from Taqman Low Density Array (TLDA, Apply Biosystems) after *Limma* Analysis. FC, fold change; COPD, chronic obstructive pulmonary disease; SK, smokers; NS, non-smokers.

Table E2. Primer used in this study

Figure E1. Graphic representation of miRNA expression changes between patients.

Figure E2. Heat map of the 8 dysregulated miRNAs. The color represents the miRNA expression measured as CT. Note that the higher the CT the lower the miRNA expression.

Figure E3. Positive and negative correlation of miR-139 and miR-485 expression (ddCt) with FEV₁ respectively by Spearman analysis.

Figure E4. Expression of miR-204 in SMC during differentiation (D0, D2 and D6) and in pulmonary artery-SMC from patients. COPD, chronic obstructive pulmonary disease; SK, smokers; NS, non-smokers.

Figure E5. Expression of IGF1 analysed by real time PCR in AS-miR-197 and scrambled transfected cells. *p< 0.05 by paired-test.

Table E1

Targets	FC			p valor		
	NS vs S	NS vs COPD	S vs COPD	NS vs S	NS vs COPD	S vs COPD
hsa-let-7a-4373169	1,048	1,386	1,322	0,958	0,739	0,649
hsa-let-7c-4373167	1,035	1,254	1,211	0,951	0,737	0,699
hsa-let-7d-4395394	-1,136	1,059	1,204	0,811	0,918	0,596
hsa-let-7e-4395517	-1,161	1,087	1,262	0,783	0,890	0,494
hsa-let-7f-4373164	-1,348	1,037	1,398	0,657	0,958	0,280
hsa-let-7g-4395393	-1,181	1,007	1,189	0,670	0,986	0,447
hsa-miR-1-4395333	1,002	1,014	1,013	0,997	0,977	0,962
hsa-miR-9-4373285	-2,206	-1,740	1,268	0,100	0,253	0,531
hsa-miR-10a-4373153	-1,454	-1,155	1,259	0,474	0,779	0,564
hsa-miR-10b-4395329	1,181	1,027	-1,150	0,683	0,946	0,707
MammU6-4395470	-1,322	1,249	1,652	0,691	0,717	0,392
MammU6-4395470	8,820	4,170	-2,115	0,421	0,610	0,697
hsa-miR-15a-4373123	-1,006	2,651	2,666	0,995	0,260	0,119
hsa-miR-15b-4373122	-2,294	-1,632	1,405	0,241	0,371	0,594
hsa-miR-16-4373121	-1,156	-1,121	1,031	0,717	0,655	0,939
hsa-miR-17-4395419	-1,326	-1,121	1,183	0,562	0,800	0,561
hsa-miR-18a-4395533	-2,320	1,025	2,378	0,266	0,973	0,119
hsa-miR-18b-4395328	1,276	1,632	1,278	0,108	0,053	0,341
hsa-miR-19a-4373099	-1,746	-1,458	1,197	0,256	0,378	0,639
hsa-miR-19b-4373098	-1,322	-1,260	1,049	0,490	0,495	0,866
hsa-miR-20a-4373286	-1,185	-1,098	1,080	0,809	0,900	0,874
hsa-miR-20b-4373263	1,053	-1,622	-1,707	0,864	0,222	0,160
hsa-miR-21-4373090	1,481	1,912	1,291	0,663	0,491	0,672
hsa-miR-22-4373079	1,368	1,084	-1,263	0,564	0,880	0,578
hsa-miR-23a-4373074	-1,530	-1,498	1,021	0,568	0,586	0,884
hsa-miR-23b-4373073	1,209	1,450	1,199	0,854	0,735	0,812
hsa-miR-24-4373072	-1,488	-1,542	-1,036	0,364	0,151	0,934
hsa-miR-25-4373071	1,350	2,256	1,671	0,779	0,458	0,487
hsa-miR-26a-4395166	-1,422	-1,234	1,152	0,355	0,536	0,645
hsa-miR-26b-4395167	-1,213	-1,292	-1,065	0,701	0,636	0,861
hsa-miR-27a-4373287	-1,070	1,080	1,156	0,880	0,858	0,599
hsa-miR-27b-4373068	1,094	1,451	1,326	0,876	0,523	0,350
hsa-miR-28-3p-4395557	-1,129	-1,076	1,049	0,752	0,821	0,864
hsa-miR-28-5p-4373067	-1,239	1,066	1,321	0,591	0,868	0,310
MammU6-4395470	-1,157	1,102	1,275	0,826	0,878	0,608
MammU6-4395470	-1,303	-1,023	1,274	0,633	0,965	0,536
hsa-miR-29a-4395223	-1,103	-1,010	1,092	0,756	0,965	0,772
hsa-miR-29b-4373288	1,202	2,291	1,906	0,823	0,301	0,174
hsa-miR-29c-4395171	-1,424	-1,521	-1,068	0,493	0,301	0,905
hsa-miR-30b-4373290	-1,327	-1,056	1,256	0,555	0,903	0,433
hsa-miR-30c-4373060	-1,096	-1,066	1,028	0,800	0,849	0,933
hsa-miR-31-4395390	3,663	1,219	-3,004	0,148	0,802	0,170
hsa-miR-32-4395220	1,178	-1,104	-1,301	0,688	0,787	0,212
hsa-miR-33b-4395196	1,276	1,224	-1,043	0,108	0,038	0,755

hsa-miR-34a-4395168	-1,079	1,663	1,794	0,919	0,356	0,339
hsa-miR-34c-5p-4373036	1,086	-1,079	-1,171	0,779	0,774	0,313
hsa-miR-92a-4395169	-1,120	1,035	1,160	0,831	0,950	0,594
hsa-miR-93-4373302	-1,218	-1,024	1,189	0,632	0,950	0,529
hsa-miR-95-4373011	-2,196	-1,763	1,245	0,172	0,104	0,682
hsa-miR-96-4373372	1,276	1,224	-1,043	0,108	0,038	0,755
hsa-miR-98-4373009	1,306	2,365	1,810	0,083	0,011	0,070
hsa-miR-99a-4373008	1,308	-1,008	-1,318	0,788	0,993	0,710
hsa-miR-99b-4373007	-1,450	-1,094	1,326	0,443	0,842	0,380
hsa-miR-100-4373160	-1,130	-1,251	-1,107	0,784	0,644	0,753
hsa-miR-101-4395364	-1,011	1,024	1,035	0,985	0,969	0,931
hsa-miR-103-4373158	-1,106	1,196	1,323	0,817	0,670	0,357
hsa-miR-105-4395278	1,276	1,224	-1,043	0,108	0,038	0,755
hsa-miR-106a-4395280	-1,260	-1,084	1,163	0,628	0,859	0,607
RNU44-4373384	1,049	1,336	1,274	0,893	0,439	0,465
hsa-miR-106b-4373155	-1,277	-1,039	1,229	0,499	0,909	0,429
hsa-miR-107-4373154	-1,008	1,154	1,164	0,986	0,751	0,665
hsa-miR-122-4395356	1,276	1,224	-1,043	0,108	0,038	0,755
hsa-miR-124-4373295	1,500	1,224	-1,226	0,103	0,038	0,377
hsa-miR-125a-3p-4395310	1,954	-1,022	-1,997	0,426	0,979	0,258
hsa-miR-125a-5p-4395309	-1,616	-1,486	1,087	0,185	0,159	0,799
hsa-miR-125b-4373148	-1,274	-1,270	1,003	0,637	0,664	0,991
hsa-miR-126-4395339	1,030	-1,013	-1,043	0,956	0,979	0,935
hsa-miR-127-3p-4373147	-1,676	-1,405	1,193	0,539	0,662	0,816
hsa-miR-127-5p-4395340	1,276	1,224	-1,043	0,108	0,038	0,755
hsa-miR-128-4395327	-1,811	-1,044	1,735	0,511	0,963	0,285
hsa-miR-129-3p-4373297	1,349	1,005	-1,343	0,488	0,989	0,380
hsa-miR-129-5p-4373171	1,276	1,224	-1,043	0,108	0,038	0,755
hsa-miR-130a-4373145	1,209	1,799	1,489	0,838	0,545	0,567
hsa-miR-130b-4373144	1,661	1,250	-1,329	0,502	0,763	0,598
hsa-miR-132-4373143	-3,778	-1,793	2,107	0,134	0,468	0,055
hsa-miR-133a-4395357	-1,127	-1,036	1,088	0,782	0,924	0,847
hsa-miR-133b-4395358	1,216	1,120	-1,085	0,672	0,792	0,848
hsa-miR-134-4373299	-1,420	-1,794	-1,263	0,450	0,343	0,624
hsa-miR-135a-4373140	1,123	1,262	1,124	0,580	0,338	0,576
hsa-miR-135b-4395372	1,655	1,681	1,015	0,453	0,425	0,981
hsa-miR-136-4373173	1,093	-1,036	-1,133	0,734	0,879	0,382
hsa-miR-137-4373301	1,276	1,224	-1,043	0,108	0,038	0,755
hsa-miR-138-4395395	-1,775	-1,488	1,193	0,502	0,469	0,806
hsa-miR-139-3p-4395424	2,059	2,038	-1,010	0,035	0,015	0,978
hsa-miR-139-5p-4395400	1,154	1,953	1,691	0,580	0,013	0,042
hsa-miR-140-3p-4395345	-1,252	-1,144	1,095	0,611	0,719	0,854
hsa-miR-140-5p-4373374	-1,037	-1,122	-1,082	0,947	0,815	0,849
hsa-miR-141-4373137	2,033	1,360	-1,495	0,305	0,610	0,454
hsa-miR-142-3p-4373136	1,860	2,621	1,409	0,286	0,124	0,409
hsa-miR-142-5p-4395359	1,612	1,140	-1,414	0,185	0,610	0,275
hsa-miR-143-4395360	1,132	1,086	-1,043	0,762	0,826	0,893

hsa-miR-145-4395389	-1,200	-1,091	1,100	0,645	0,816	0,747
hsa-miR-146a-4373132	-1,292	1,106	1,428	0,421	0,699	0,234
hsa-miR-146b-3p-4395472	1,510	1,422	-1,062	0,110	0,048	0,825
hsa-miR-146b-5p-4373178	1,041	2,842	2,731	0,922	0,014	0,021
hsa-miR-147b-4395373	1,276	1,224	-1,043	0,108	0,038	0,755
hsa-miR-148a-4373130	-1,423	-1,070	1,331	0,447	0,884	0,478
hsa-miR-148b-4373129	1,662	1,663	1,001	0,497	0,497	0,999
hsa-miR-149-4395366	-1,276	-2,411	-1,889	0,498	0,036	0,138
hsa-miR-150-4373127	1,061	1,284	1,210	0,903	0,502	0,670
hsa-miR-152-4395170	-1,576	-1,568	1,005	0,223	0,123	0,988
hsa-miR-153-4373305	1,276	1,224	-1,043	0,108	0,038	0,755
hsa-miR-154-4373270	1,276	1,224	-1,043	0,108	0,038	0,755
hsa-miR-181a-4373117	1,597	-1,091	-1,743	0,205	0,787	0,064
hsa-miR-181c-4373115	1,276	1,224	-1,043	0,108	0,038	0,755
hsa-miR-182-4395445	1,610	1,170	-1,376	0,055	0,206	0,151
RNU48-4373383	-1,575	1,032	1,626	0,248	0,925	0,183
hsa-miR-183-4395380	1,276	1,224	-1,043	0,108	0,038	0,755
hsa-miR-184-4373113	-2,689	-1,090	2,466	0,226	0,915	0,105
hsa-miR-185-4395382	2,879	2,383	-1,208	0,238	0,334	0,636
hsa-miR-186-4395396	-1,469	-1,431	1,027	0,278	0,116	0,937
hsa-miR-187-4373307	1,600	1,542	-1,037	0,422	0,415	0,944
hsa-miR-188-3p-4395217	1,276	1,224	-1,043	0,108	0,038	0,755
hsa-miR-190-4373110	-2,733	-1,161	2,355	0,227	0,855	0,114
hsa-miR-191-4395410	-1,073	1,136	1,218	0,763	0,558	0,303
hsa-miR-192-4373108	-1,517	1,207	1,831	0,625	0,774	0,373
hsa-miR-193a-3p-4395361	1,083	-1,036	-1,121	0,819	0,907	0,772
hsa-miR-193a-5p-4395392	3,870	1,964	-1,971	0,266	0,580	0,283
hsa-miR-193b-4395478	-1,248	-1,226	1,019	0,533	0,324	0,960
hsa-miR-194-4373106	1,285	1,002	-1,282	0,662	0,997	0,538
hsa-miR-195-4373105	-1,588	-1,357	1,170	0,273	0,401	0,682
hsa-miR-196b-4395326	-1,626	1,297	2,109	0,332	0,565	0,164
hsa-miR-197-4373102	-1,673	-3,180	-1,901	0,348	0,033	0,144
hsa-miR-198-4395384	1,427	1,224	-1,165	0,121	0,038	0,469
hsa-miR-199a-5p-4373272	2,780	2,929	1,054	0,118	0,105	0,912
hsa-miR-199a-3p-4395415	-1,657	-1,539	1,077	0,223	0,278	0,792
hsa-miR-199b-5p-4373100	-1,075	1,108	1,191	0,804	0,737	0,371
hsa-miR-200a-4378069	1,992	-1,389	-2,768	0,389	0,663	0,099
hsa-miR-200b-4395362	1,275	1,018	-1,252	0,630	0,971	0,502
hsa-miR-200c-4395411	2,604	1,375	-1,894	0,123	0,630	0,287
hsa-miR-202-4395474	1,618	1,224	-1,322	0,083	0,038	0,280
hsa-miR-203-4373095	-1,586	-1,951	-1,230	0,618	0,465	0,689
hsa-miR-204-4373094	-1,783	-1,704	1,047	0,097	0,034	0,884
hsa-miR-205-4373093	1,730	1,822	1,053	0,045	0,020	0,870
hsa-miR-208b-4395401	1,276	1,224	-1,043	0,108	0,038	0,755
hsa-miR-210-4373089	-1,378	-1,439	-1,045	0,586	0,357	0,941
hsa-miR-214-4395417	-1,204	-1,065	1,130	0,601	0,842	0,709
hsa-miR-215-4373084	1,276	1,295	1,015	0,108	0,019	0,918

hsa-miR-216a-4395331	-2,617	-1,122	2,332	0,095	0,833	0,059
hsa-miR-216b-4395437	1,276	1,382	1,083	0,108	0,041	0,654
hsa-miR-217-4395448	1,176	1,407	1,197	0,694	0,437	0,539
hsa-miR-218-4373081	-1,256	-1,128	1,113	0,521	0,619	0,725
hsa-miR-219-5p-4373080	1,276	1,224	-1,043	0,108	0,038	0,755
hsa-miR-221-4373077	1,311	1,625	1,239	0,796	0,643	0,764
hsa-miR-222-4395387	-1,565	-1,539	1,017	0,207	0,225	0,954
hsa-miR-223-4395406	1,250	1,441	1,153	0,620	0,316	0,770
hsa-miR-224-4395210	-1,671	1,343	2,243	0,406	0,611	0,151
hsa-miR-296-3p-4395212	1,276	1,224	-1,043	0,108	0,038	0,755
hsa-miR-296-5p-4373066	1,186	1,138	-1,043	0,266	0,208	0,755
hsa-miR-299-3p-4373189	1,276	1,522	1,192	0,108	0,090	0,491
hsa-miR-299-5p-4373188	1,068	1,025	-1,043	0,758	0,894	0,755
hsa-miR-301a-4373064	-1,840	-1,522	1,209	0,347	0,445	0,732
hsa-miR-301b-4395503	1,080	1,044	-1,035	0,831	0,902	0,855
hsa-miR-302a-4378070	1,276	1,224	-1,043	0,108	0,038	0,755
ath-miR159a-4373390	1,276	1,224	-1,043	0,108	0,038	0,755
hsa-miR-302b-4378071	1,276	1,224	-1,043	0,108	0,038	0,755
hsa-miR-302c-4378072	1,276	1,224	-1,043	0,108	0,038	0,755
hsa-miR-320-4395388	-1,141	-1,100	1,037	0,615	0,606	0,891
hsa-miR-323-3p-4395338	-2,010	-1,874	1,073	0,302	0,342	0,858
hsa-miR-324-3p-4395272	-1,141	-1,112	1,026	0,689	0,718	0,935
hsa-miR-324-5p-4373052	-3,147	-3,049	1,032	0,504	0,516	0,955
hsa-miR-326-4373050	1,276	1,224	-1,043	0,108	0,038	0,755
hsa-miR-328-4373049	1,127	-1,361	-1,534	0,712	0,446	0,195
hsa-miR-329-4373191	1,276	1,224	-1,043	0,108	0,038	0,755
hsa-miR-330-3p-4373047	1,276	1,224	-1,043	0,108	0,038	0,755
hsa-miR-330-5p-4395341	1,276	1,224	-1,043	0,108	0,038	0,755
hsa-miR-331-3p-4373046	-1,279	-1,827	-1,429	0,627	0,168	0,494
hsa-miR-331-5p-4395344	3,297	1,805	-1,827	0,005	0,090	0,136
hsa-miR-335-4373045	-1,876	-1,225	1,531	0,299	0,721	0,337
hsa-miR-337-5p-4395267	-1,035	-1,795	-1,734	0,961	0,375	0,301
hsa-miR-338-3p-4395363	-1,217	-1,096	1,110	0,710	0,851	0,765
hsa-miR-339-3p-4395295	1,067	-1,570	-1,675	0,910	0,428	0,329
hsa-miR-339-5p-4395368	-1,127	-1,337	-1,187	0,850	0,637	0,674
hsa-miR-340-4395369	-1,303	-1,322	-1,015	0,479	0,435	0,966
has-miR-155-4395459	-1,212	-1,130	1,073	0,599	0,692	0,846
hsa-let-7b-4395446	1,219	1,444	1,184	0,809	0,701	0,832
hsa-miR-342-3p-4395371	-1,361	-1,203	1,131	0,445	0,575	0,766
hsa-miR-342-5p-4395258	1,276	1,224	-1,043	0,108	0,038	0,755
hsa-miR-345-4395297	-1,717	-1,113	1,543	0,245	0,674	0,320
hsa-miR-361-5p-4373035	-2,406	1,425	3,428	0,180	0,586	0,024
hsa-miR-362-3p-4395228	-1,454	1,102	1,603	0,536	0,872	0,308
hsa-miR-362-5p-4378092	-1,161	-1,455	-1,253	0,813	0,548	0,647
hsa-miR-363-4378090	-1,046	1,076	1,125	0,884	0,824	0,587
hsa-miR-365-4373194	-1,390	-1,201	1,157	0,538	0,721	0,645
hsa-miR-367-4373034	1,276	1,224	-1,043	0,108	0,038	0,755

hsa-miR-369-3p-4373032	1,276	1,224	-1,043	0,108	0,038	0,755
hsa-miR-369-5p-4373195	-1,346	-1,738	-1,292	0,608	0,324	0,293
hsa-miR-370-4395386	-2,203	-1,683	1,309	0,350	0,540	0,644
hsa-miR-371-3p-4395235	1,276	1,224	-1,043	0,108	0,038	0,755
hsa-miR-372-4373029	-1,251	-1,293	-1,034	0,591	0,524	0,895
hsa-miR-373-4378073	1,276	1,224	-1,043	0,108	0,038	0,755
hsa-miR-374a-4373028	-1,305	-1,378	-1,056	0,443	0,424	0,866
hsa-miR-374b-4381045	-1,369	-1,412	-1,031	0,405	0,237	0,933
hsa-miR-375-4373027	1,009	1,247	1,236	0,991	0,776	0,728
hsa-miR-376a-4373026	-1,648	-1,293	1,275	0,379	0,625	0,589
hsa-miR-376b-4373196	1,276	1,224	-1,043	0,108	0,038	0,755
hsa-miR-377-4373025	1,276	1,224	-1,043	0,108	0,038	0,755
hsa-miR-379-4373349	-2,478	-1,391	1,782	0,335	0,714	0,375
hsa-miR-380-4373022	1,276	1,224	-1,043	0,108	0,038	0,755
hsa-miR-381-4373020	1,276	1,224	-1,043	0,108	0,038	0,755
hsa-miR-382-4373019	1,276	1,224	-1,043	0,108	0,038	0,755
hsa-miR-383-4373018	1,754	-1,114	-1,954	0,272	0,726	0,130
hsa-miR-409-5p-4395442	1,276	1,224	-1,043	0,108	0,038	0,755
hsa-miR-410-4378093	-3,049	-2,488	1,226	0,029	0,091	0,655
hsa-miR-411-4381013	-3,321	-1,802	1,843	0,082	0,223	0,290
hsa-miR-422a-4395408	-1,419	-1,094	1,297	0,446	0,841	0,539
hsa-miR-423-5p-4395451	-1,250	-1,215	1,029	0,747	0,787	0,960
hsa-miR-424-4373201	1,124	1,079	-1,043	0,500	0,568	0,755
hsa-miR-425-4380926	1,168	1,396	1,195	0,810	0,495	0,737
hsa-miR-429-4373203	-3,358	-1,721	1,951	0,007	0,240	0,153
hsa-miR-431-4395173	1,276	1,224	-1,043	0,108	0,038	0,755
hsa-miR-433-4373205	2,373	1,082	-2,194	0,289	0,916	0,194
hsa-miR-449a-4373207	1,159	-1,380	-1,600	0,871	0,729	0,335
hsa-miR-449b-4381011	1,165	1,139	-1,023	0,754	0,778	0,945
hsa-miR-450a-4395414	1,276	1,224	-1,043	0,108	0,038	0,755
hsa-miR-450b-3p-4395319	1,276	1,224	-1,043	0,108	0,038	0,755
hsa-miR-450b-5p-4395318	1,276	1,224	-1,043	0,108	0,038	0,755
hsa-miR-451-4373360	3,238	5,267	1,626	0,229	0,063	0,526
hsa-miR-452-4395440	-1,150	1,169	1,344	0,827	0,758	0,607
hsa-miR-453-4395429	1,276	1,224	-1,043	0,108	0,038	0,755
hsa-miR-454-4395434	-1,298	-1,258	1,032	0,419	0,483	0,916
hsa-miR-455-3p-4395355	-1,522	1,471	2,240	0,650	0,680	0,183
hsa-miR-455-5p-4378098	-1,323	-1,249	1,060	0,587	0,656	0,896
hsa-miR-483-5p-4395449	1,488	1,471	-1,012	0,330	0,326	0,975
hsa-miR-484-4381032	-1,305	-1,467	-1,124	0,612	0,379	0,803
hsa-miR-485-3p-4378095	-2,501	-3,380	-1,352	0,136	0,057	0,301
hsa-miR-485-5p-4373212	1,276	1,224	-1,043	0,108	0,038	0,755
hsa-miR-486-3p-4395204	-1,457	-1,827	-1,254	0,565	0,305	0,739
hsa-miR-486-5p-4378096	1,534	-1,064	-1,632	0,267	0,869	0,210
hsa-miR-487a-4378097	1,276	1,224	-1,043	0,108	0,038	0,755
hsa-miR-487b-4378102	-2,635	-2,738	-1,039	0,049	0,040	0,936
hsa-miR-488-4395468	1,276	1,224	-1,043	0,108	0,038	0,755

hsa-miR-489-4395469	-1,485	-1,197	1,240	0,217	0,508	0,312
hsa-miR-490-3p-4373215	1,276	1,224	-1,043	0,108	0,038	0,755
hsa-miR-491-3p-4395471	1,376	1,224	-1,124	0,047	0,038	0,403
hsa-miR-491-5p-4381053	-1,615	-1,859	-1,151	0,400	0,148	0,801
hsa-miR-493-4395475	-1,375	1,017	1,399	0,602	0,977	0,480
hsa-miR-494-4395476	-1,424	-1,105	1,289	0,666	0,905	0,683
hsa-miR-495-4381078	-3,005	-3,137	-1,044	0,194	0,187	0,926
hsa-miR-496-4386771	1,276	1,224	-1,043	0,108	0,038	0,755
hsa-miR-499-3p-4395538	1,276	1,224	-1,043	0,108	0,038	0,755
hsa-miR-499-5p-4381047	1,276	2,082	1,632	0,108	0,055	0,195
hsa-miR-500-4395539	-1,843	1,488	2,743	0,414	0,580	0,064
hsa-miR-501-3p-4395546	1,062	1,019	-1,043	0,764	0,911	0,755
hsa-miR-501-5p-4373226	-2,550	-1,098	2,322	0,076	0,839	0,039
hsa-miR-502-3p-4395194	-2,549	-1,239	2,057	0,072	0,666	0,036
hsa-miR-502-5p-4373227	1,632	2,154	1,319	0,332	0,151	0,574
hsa-miR-503-4373228	1,042	-1,207	-1,258	0,925	0,632	0,298
hsa-miR-504-4395195	1,177	1,218	1,034	0,840	0,792	0,959
hsa-miR-505-4395200	1,769	1,224	-1,446	0,077	0,038	0,224
hsa-miR-507-4373232	1,276	1,224	-1,043	0,108	0,038	0,755
hsa-miR-508-3p-4373233	-1,868	-1,821	1,026	0,587	0,604	0,933
hsa-miR-508-5p-4395203	1,276	1,224	-1,043	0,108	0,038	0,755
hsa-miR-509-5p-4395346	1,276	1,224	-1,043	0,108	0,038	0,755
hsa-miR-510-4395352	1,276	1,224	-1,043	0,108	0,038	0,755
hsa-miR-512-3p-4381034	-2,160	-2,252	-1,043	0,318	0,292	0,755
hsa-miR-512-5p-4373238	1,276	1,224	-1,043	0,108	0,038	0,755
hsa-miR-513-5p-4395201	1,276	1,224	-1,043	0,108	0,038	0,755
hsa-miR-515-3p-4395480	1,276	1,224	-1,043	0,108	0,038	0,755
hsa-miR-515-5p-4373242	1,276	1,224	-1,043	0,108	0,038	0,755
hsa-miR-516a-5p-4395527	1,276	1,224	-1,043	0,108	0,038	0,755
hsa-miR-516b-4395172	1,276	1,224	-1,043	0,108	0,038	0,755
hsa-miR-517a-4395513	1,276	1,224	-1,043	0,108	0,038	0,755
hsa-miR-517c-4373264	1,201	1,190	-1,010	0,219	0,085	0,945
hsa-miR-518a-3p-4395508	1,276	1,224	-1,043	0,108	0,038	0,755
hsa-miR-518a-5p-4395507	1,276	1,224	-1,043	0,108	0,038	0,755
hsa-miR-518b-4373246	1,149	1,133	-1,014	0,600	0,615	0,939
hsa-miR-518c-4395512	-3,271	-3,410	-1,043	0,454	0,439	0,755
hsa-miR-518d-3p-4373248	1,276	1,827	1,432	0,108	0,143	0,382
hsa-miR-518d-5p-4395500	1,276	1,224	-1,043	0,108	0,038	0,755
hsa-miR-518e-4395506	-1,019	-1,062	-1,043	0,949	0,821	0,755
hsa-miR-518f-4395499	1,276	1,224	-1,043	0,108	0,038	0,755
hsa-miR-519a-4395526	1,285	1,224	-1,050	0,092	0,038	0,707
hsa-miR-519d-4395514	1,471	1,329	-1,107	0,096	0,012	0,638
hsa-miR-519e-4395481	-1,121	-1,169	-1,043	0,787	0,705	0,755
hsa-miR-520a-3p-4373268	1,276	1,224	-1,043	0,108	0,038	0,755
hsa-miR-520a-5p-4378085	1,276	1,224	-1,043	0,108	0,038	0,755
hsa-miR-520d-5p-4395504	1,276	1,224	-1,043	0,108	0,038	0,755
hsa-miR-520g-4373257	1,276	1,224	-1,043	0,108	0,038	0,755

hsa-miR-521-4373259	1,276	1,224	-1,043	0,108	0,038	0,755
hsa-miR-522-4395524	-1,099	1,288	1,415	0,793	0,517	0,144
hsa-miR-523-4395497	-1,058	-1,103	-1,043	0,861	0,747	0,755
hsa-miR-524-5p-4395174	1,276	1,224	-1,043	0,108	0,038	0,755
hsa-miR-525-3p-4395496	1,044	1,053	1,009	0,854	0,806	0,948
hsa-miR-525-5p-4378088	1,276	1,224	-1,043	0,108	0,038	0,755
hsa-miR-526b-4395493	1,276	1,224	-1,043	0,108	0,038	0,755
hsa-miR-532-3p-4395466	-1,315	1,149	1,510	0,384	0,612	0,082
hsa-miR-532-5p-4380928	-1,588	1,014	1,610	0,543	0,982	0,385
hsa-miR-539-4378103	1,075	-1,249	-1,343	0,936	0,805	0,657
hsa-miR-541-4395312	1,276	1,224	-1,043	0,108	0,038	0,755
hsa-miR-542-3p-4378101	1,276	1,344	1,053	0,108	0,024	0,742
hsa-miR-542-5p-4395351	-8,522	-6,855	1,243	0,385	0,433	0,441
hsa-miR-544-4395376	1,276	1,224	-1,043	0,108	0,038	0,755
hsa-miR-545-4395378	2,029	1,660	-1,222	0,025	0,111	0,549
hsa-miR-548a-3p-4380948	1,276	2,829	2,217	0,108	0,250	0,375
hsa-miR-548a-5p-4395523	2,813	1,224	-2,298	0,216	0,038	0,310
hsa-miR-548b-3p-4380951	1,276	1,224	-1,043	0,108	0,038	0,755
hsa-miR-548b-5p-4395519	1,276	1,224	-1,043	0,108	0,038	0,755
hsa-miR-548c-3p-4380993	1,276	1,224	-1,043	0,108	0,038	0,755
hsa-miR-548c-5p-4395540	-1,069	-1,115	-1,043	0,840	0,731	0,755
hsa-miR-548d-3p-4381008	1,276	1,224	-1,043	0,108	0,038	0,755
hsa-miR-548d-5p-4395348	1,289	1,224	-1,053	0,091	0,038	0,694
hsa-miR-551b-4380945	-3,749	-3,908	-1,043	0,449	0,435	0,755
hsa-miR-556-3p-4395456	1,276	1,224	-1,043	0,108	0,038	0,755
hsa-miR-556-5p-4395455	-5,350	-4,663	1,147	0,417	0,454	0,536
hsa-miR-561-4380938	1,276	1,224	-1,043	0,108	0,038	0,755
hsa-miR-570-4395458	1,486	1,224	-1,214	0,026	0,038	0,214
hsa-miR-574-3p-4395460	-1,636	-1,252	1,307	0,162	0,382	0,392
hsa-miR-576-3p-4395462	-1,135	1,178	1,337	0,742	0,697	0,249
hsa-miR-576-5p-4395461	1,553	1,299	-1,196	0,037	0,014	0,344
hsa-miR-579-4395509	-1,135	1,029	1,168	0,742	0,944	0,477
hsa-miR-582-3p-4395510	1,276	1,224	-1,043	0,108	0,038	0,755
hsa-miR-582-5p-4395175	1,238	1,012	-1,224	0,565	0,969	0,427
hsa-miR-589-4395520	1,276	1,224	-1,043	0,108	0,038	0,755
hsa-miR-590-5p-4395176	-1,264	-1,101	1,148	0,611	0,801	0,727
hsa-miR-597-4380960	-1,152	1,047	1,207	0,788	0,935	0,569
hsa-miR-598-4395179	1,220	1,020	-1,196	0,821	0,983	0,779
hsa-miR-615-3p-4386777	1,276	1,224	-1,043	0,108	0,038	0,755
hsa-miR-615-5p-4395464	1,276	1,224	-1,043	0,108	0,038	0,755
hsa-miR-616-4395525	1,276	1,224	-1,043	0,108	0,038	0,755
hsa-miR-618-4380996	1,276	1,271	-1,004	0,108	0,022	0,978
hsa-miR-624-4395541	1,276	1,224	-1,043	0,108	0,038	0,755
hsa-miR-625-4395542	-1,018	1,048	1,067	0,945	0,856	0,706
hsa-miR-627-4380967	-1,789	-2,272	-1,270	0,257	0,113	0,416
hsa-miR-628-5p-4395544	-1,261	-1,362	-1,081	0,389	0,116	0,796
hsa-miR-629-4395547	1,512	1,224	-1,235	0,066	0,038	0,303

hsa-miR-636-4395199	-2,731	-2,625	1,040	0,108	0,119	0,922
hsa-miR-642-4380995	1,276	1,533	1,201	0,108	0,068	0,450
hsa-miR-651-4381007	1,276	1,224	-1,043	0,108	0,038	0,755
hsa-miR-652-4395463	-2,128	-1,959	1,086	0,071	0,113	0,859
hsa-miR-653-4395403	1,276	1,224	-1,043	0,108	0,038	0,755
hsa-miR-654-3p-4395350	1,276	1,224	-1,043	0,108	0,038	0,755
hsa-miR-654-5p-4381014	1,276	1,224	-1,043	0,108	0,038	0,755
hsa-miR-655-4381015	1,194	1,255	1,051	0,483	0,383	0,854
hsa-miR-660-4380925	-1,277	-1,205	1,060	0,568	0,565	0,878
hsa-miR-671-3p-4395433	-1,218	1,464	1,783	0,811	0,645	0,336
hsa-miR-672-4395438	1,276	1,224	-1,043	0,108	0,038	0,755
hsa-miR-674-4395193	4,275	1,224	-3,493	0,274	0,038	0,341
hsa-miR-708-4395452	-1,758	1,002	1,762	0,409	0,996	0,340
hsa-miR-744-4395435	-1,676	-1,483	1,130	0,173	0,197	0,741
hsa-miR-758-4395180	-1,749	-1,824	-1,043	0,334	0,297	0,755
hsa-miR-871-4395465	1,276	1,224	-1,043	0,108	0,038	0,755
hsa-miR-872-4395375	1,276	1,224	-1,043	0,108	0,038	0,755
hsa-miR-873-4395467	1,276	1,224	-1,043	0,108	0,038	0,755
hsa-miR-874-4395379	1,843	1,938	1,051	0,101	0,253	0,929
hsa-miR-875-3p-4395315	-1,723	-1,796	-1,043	0,545	0,513	0,755
hsa-miR-876-3p-4395336	1,276	1,224	-1,043	0,108	0,038	0,755
hsa-miR-876-5p-4395316	1,276	1,224	-1,043	0,108	0,038	0,755
hsa-miR-885-3p-4395483	-5,463	-5,695	-1,043	0,414	0,403	0,755
hsa-miR-885-5p-4395407	1,024	-1,172	-1,200	0,972	0,814	0,745
hsa-miR-886-3p-4395305	-1,130	-1,186	-1,049	0,842	0,668	0,937
hsa-miR-886-5p-4395304	1,084	-1,119	-1,212	0,836	0,747	0,550
hsa-miR-887-4395485	1,784	1,643	-1,086	0,373	0,434	0,878
hsa-miR-888-4395323	1,276	1,258	-1,015	0,108	0,023	0,913
hsa-miR-889-4395313	1,276	1,224	-1,043	0,108	0,038	0,755
hsa-miR-890-4395320	1,276	1,224	-1,043	0,108	0,038	0,755
hsa-miR-891a-4395302	-1,073	1,001	1,075	0,854	0,997	0,688
hsa-miR-891b-4395321	1,276	1,224	-1,043	0,108	0,038	0,755
hsa-miR-892a-4395306	1,276	1,224	-1,043	0,108	0,038	0,755
hsa-miR-147-4373131	1,276	1,224	-1,043	0,108	0,038	0,755
hsa-miR-208-4373091	1,276	1,224	-1,043	0,108	0,038	0,755
hsa-miR-211-4373088	1,276	1,224	-1,043	0,108	0,038	0,755
hsa-miR-212-4373087	-1,826	1,117	2,041	0,536	0,907	0,046
hsa-miR-219-1-3p-4395206	1,276	1,406	1,101	0,108	0,055	0,619
hsa-miR-219-2-3p-4395501	1,276	1,224	-1,043	0,108	0,038	0,755
hsa-miR-220-4373078	1,276	1,224	-1,043	0,108	0,038	0,755
hsa-miR-220b-4395317	1,276	1,224	-1,043	0,108	0,038	0,755
hsa-miR-220c-4395322	1,276	1,224	-1,043	0,108	0,038	0,755
hsa-miR-298-4395301	3,901	1,224	-3,187	0,248	0,038	0,320
hsa-miR-325-4373051	1,276	1,224	-1,043	0,108	0,038	0,755
hsa-miR-346-4373038	1,276	1,224	-1,043	0,108	0,038	0,755
hsa-miR-376c-4395233	-1,990	-1,424	1,397	0,155	0,367	0,430
hsa-miR-384-4373017	1,276	1,224	-1,043	0,108	0,038	0,755

hsa-miR-412-4373199	1,957	1,224	-1,599	0,152	0,038	0,299
hsa-miR-448-4373206	1,276	1,224	-1,043	0,108	0,038	0,755
hsa-miR-492-4373217	1,276	1,224	-1,043	0,108	0,038	0,755
hsa-miR-506-4373231	1,276	1,224	-1,043	0,108	0,038	0,755
hsa-miR-509-3-5p-4395266	1,276	1,224	-1,043	0,108	0,038	0,755
hsa-miR-511-4373236	-1,909	1,366	2,607	0,366	0,538	0,202
hsa-miR-517b-4373244	1,060	1,017	-1,043	0,790	0,930	0,755
hsa-miR-519c-3p-4373251	1,276	1,224	-1,043	0,108	0,038	0,755
hsa-miR-520b-4373252	1,276	1,224	-1,043	0,108	0,038	0,755
hsa-miR-520e-4373255	1,276	1,224	-1,043	0,108	0,038	0,755
hsa-miR-520f-4373256	1,276	1,224	-1,043	0,108	0,038	0,755

Table E2. Primers sequences 5'-3'

Gene	Sequence
Calponin F	CACGACATTTTTGAGGCCAA
Calponin R	TTTCCTTTCGTCTTCGCCAT
Sm22v2 F	GGAAGCCTTCTTTCCCCAGA
Sm22v2 R	TCCAGCTCCTCGTCATACTTCTT
MyoCD F	GCACCAAGCTCAGCTTAAGGA
MyoCD R	TGGGAGTGGGCCTGGTTT
GAPDH F	CATCACCATCTTCCAGGAGC
GAPDH R	TGGACTCCACGACGTACTIONA
β actin F	CGGAACGCCTCATTGCC
β actin R	ACCCACACTGTGCCCATCTA
Ki67 F	GCAGCCTTAACTGTGACACTTGC
Ki67 R	GCCACCGTGCCCTGG
E2F1 F	GAGAACAGGGCCACTGACTC
E2F1 R	GTTCTTGCTCCAGGCTGAGT
IGF1 F	GTGGAGACAGGGGCTTTTATT
IGF1 R	CTCCAGCCTCCTTAGATCACA

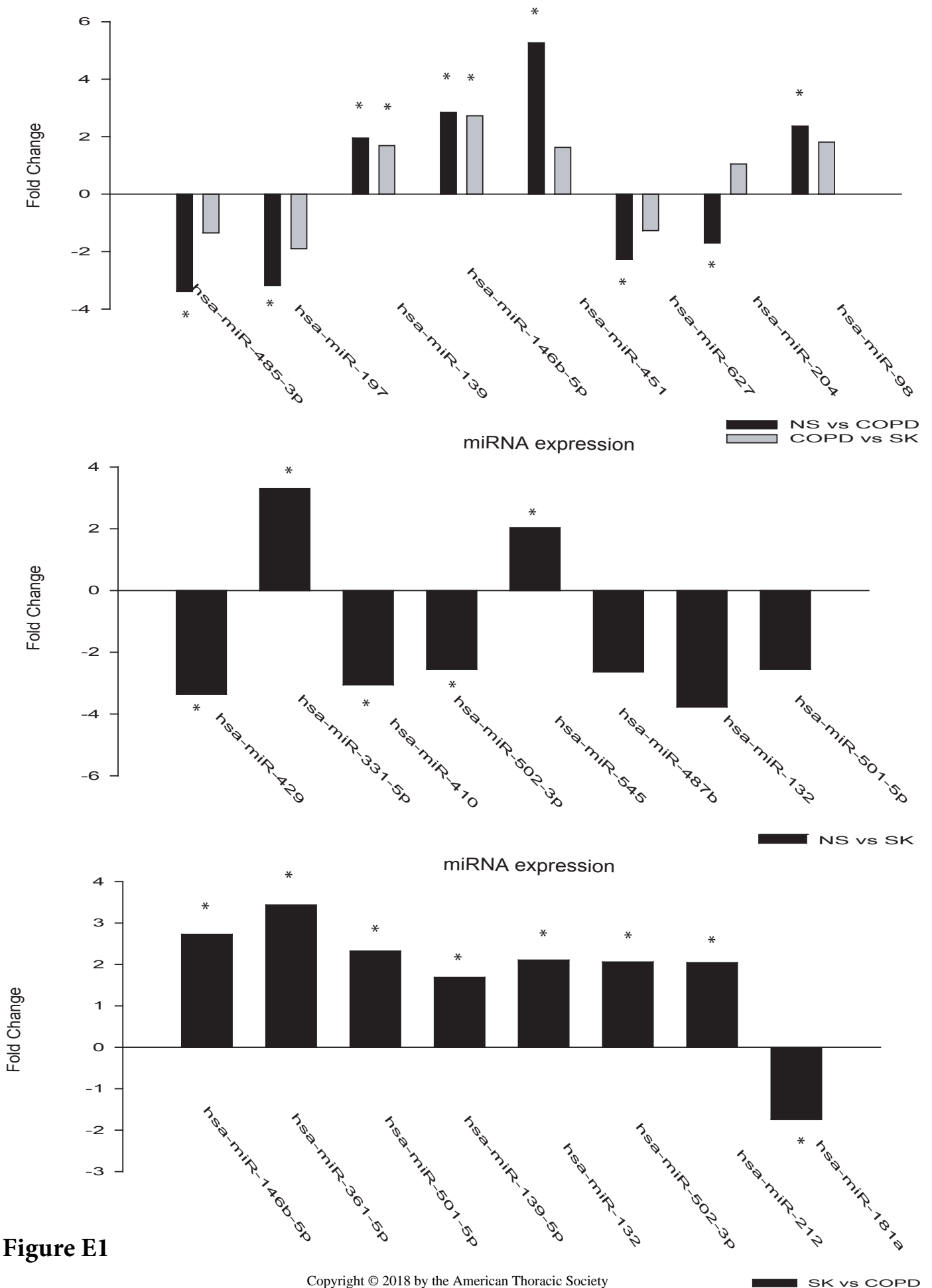


Figure E1

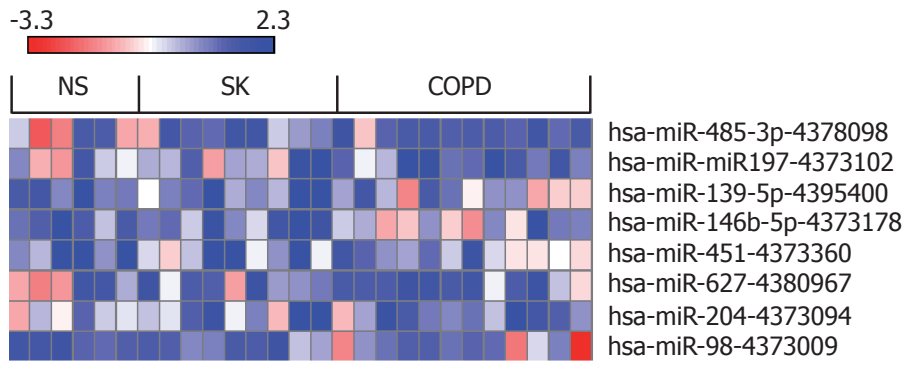


Figure E2

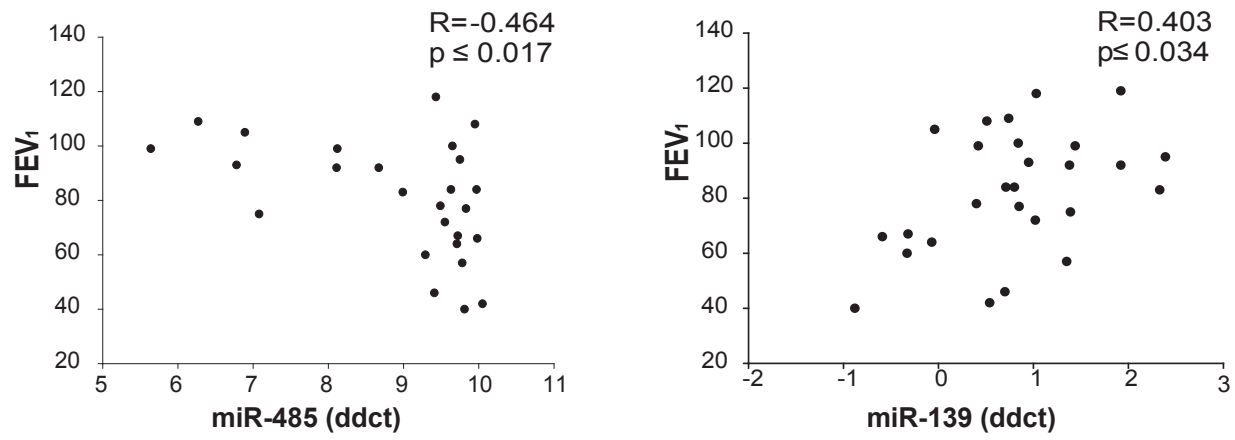


Figure E3

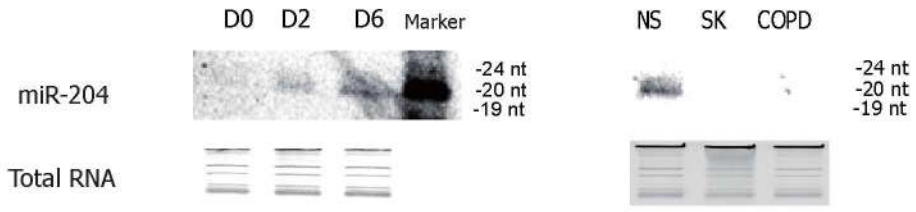


Figure E4

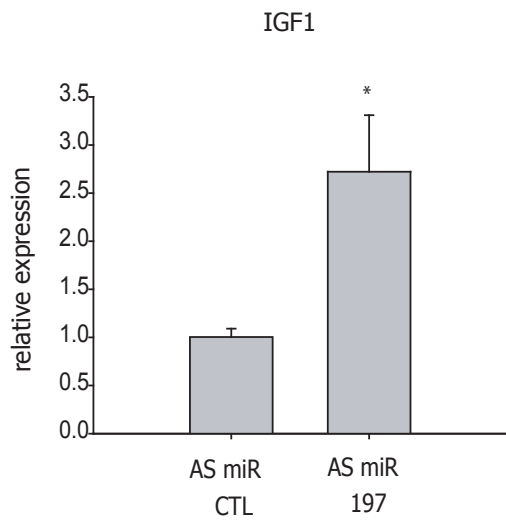


Figure E5